

The Pennsylvania State University

The Graduate School

College of Engineering

**TRANSIENT STRUCTURAL ANALYSES USING FREQUENCY-DOMAIN
COMPUTATIONS AND FOURIER TRANSFORM TECHNIQUES**

A Thesis in

Acoustics

by

Daniel J. Turkosz

© 2010 Daniel J. Turkosz

Submitted in Partial Fulfillment
of the Requirements
for the Degree of

Master of Science

May 2010

The thesis of Daniel J. Turkosz was reviewed and approved* by the following:

John B. Fahnline
Assistant Professor of Acoustics
Thesis Advisor

Stephen Hambric
Professor of Acoustics

Amanda Hanford
Special Signatory

Victor W. Sparrow
Professor of Acoustics
Interim Chair of the Graduate Program in Acoustics

*Signatures are on file in the Graduate School.

ABSTRACT

Structural-acoustic calculations are most often performed in the frequency-domain assuming time-harmonic (i.e. steady-state) forcing functions. While frequency-domain modeling can be used for most calculations, some problems in engineering and acoustics are inherently transient. In these cases, it becomes important to model the response of the structure in the time-domain, a task that can be difficult given existing frequency-domain solution infrastructure and certain frequency-domain specific types of damping. The purpose of this thesis is to establish techniques and guidelines for frequency-domain analyses by documenting time-domain solution accuracy for frequency-domain data transformed using the Fourier Transform. These guidelines have been developed by comparing time-domain solutions that are known to be accurate with transformed frequency-domain calculations first for a simple spring mass system, and then a more complex system where the finite element method is used to compute the response.

The primary guidelines involve setting frequency range and frequency resolution to values that are computationally efficient, yet still produce accurate results once transformed into the time-domain. Frequency range must be set based on the highest modal frequency of interest so its waveform is well resolved in the time-domain. Frequency resolution is tied directly to the damping of the system. The sharpest modal peak in a frequency-domain response will dictate frequency resolution, which will be set to produce accurate time-domain amplitudes. Computational savings will come mostly from limiting the modal frequency analysis range and zero-padding portions of the linear spectrum, sacrificing total sample duration in the final time-domain response and interpolating rather than directly computing certain parts of the frequency-domain response. These techniques allow for transient problems to be solved using frequency-domain results without having to create new time-domain specific analysis programs.

TABLE OF CONTENTS

List of Figures.....	v
List of Tables.....	ix
Chapter 1. INTRODUCTION.....	1
Chapter 2. BASICS OF THE ANALYSIS METHOD.....	4
Time-Domain Analyses.....	4
Frequency-Domain Analyses.....	9
Preparing Data for Comparative Analysis.....	10
Chapter 3. SPRING MASS SYSTEM ANALYSIS.....	14
Chapter 4. ANALYSES FOR FINITE ELEMENT MODELS.....	24
Chapter 5. OTHER CONSIDERATIONS.....	40
Possible Effects of a Larger Frequency Resolution.....	40
Further Reduction of Computation Times.....	44
Extended Period.....	47
Chapter 6. CONCLUSIONS.....	50
References.....	53
Appendix A: Summary of Transformed Frequency-Domain Solution Guidelines	54
Appendix B: Matlab Code.....	55
Appendix C: NASTRAN Input Deck for Figure 2.4 Time Analysis.....	56
Appendix D: NASTRAN Input Deck for Example Frequency Analysis.....	57

List of Figures

Fig.	Page	Caption
2.1	5	The first 0.04 seconds of the analytical solution for the damped spring mass system as calculated by Matlab.
2.2	6	Femap model of the spring mass system, a fixed point and a mass connected by a spring property.
2.3	6	Graphical representation of the time-domain forcing function used in Femap.
2.4	8	Femap time-domain analysis of spring mass system previously calculated analytically in Figure 2.1.
2.5	8	Comparison plot of the analytical response to the Femap response of the same system.
2.6	9	Viscous damping function for Femap frequency-domain analysis of a spring mass system.
2.7	10	Forcing function for Femap frequency-domain analysis of a spring mass system.
2.8	11	Graphical representation of the time-domain forcing function used in Femap.
2.9	12	Graphical representation of taking the complex conjugate of frequency data, mirroring it across the x-axis, and then tagging the new series onto the end of the original data series, thus forming the full linear spectrum.
3.1	14	Transformed frequency-domain representation with 1000 Hz frequency range and modal frequency of 100 Hz, compared to Femap time-domain representation.
3.2	15	Transformed frequency-domain representation with 2000 Hz frequency range and modal frequency of 100 Hz, compared to Femap time-domain representation.
3.3	15	Transformed frequency-domain representation with 1600 Hz frequency range and modal frequency of 100 Hz, compared to Femap time-domain representation.

Fig.	Page	Caption
3.4	18	Transformed frequency-domain representation with 95 Hz modal frequency, 1600 Hz frequency range and 10 Hz frequency resolution, compared to Femap time-domain representation.
3.5	19	Transformed frequency-domain representation with 96.3 Hz modal frequency, 1600 Hz frequency range and 14.8 Hz frequency resolution, compared to Femap time-domain representation.
3.6	19	Transformed frequency-domain representation with 90 Hz modal frequency, 1600 Hz frequency range and 20 Hz frequency resolution, compared to Femap time-domain representation.
3.7	20	Transformed frequency-domain representation with 98.75 Hz modal frequency, 1600 Hz frequency range and 2.5 Hz frequency resolution, compared to Femap time-domain representation.
3.8	21	Transformed frequency-domain representation with 97.5 Hz modal frequency, 1600 Hz frequency range and 5 Hz frequency resolution, compared to Femap time-domain representation.
3.9	21	Transformed frequency-domain representation with 95 Hz modal frequency, 1600 Hz frequency range and 10 Hz frequency resolution, compared to Femap time-domain representation.
4.1	24	Femap “hinge plate” model, broken into 288 nodes with 240 elements.
4.2	26	Deformed and contoured representations of the mode shapes for the first three modes of vibration of the hinge plate.
4.3	27	Representation of the time-domain forcing function for the hinge plate.
4.4	28	Hinge plate model shown with constraints around the hole and forcing function at node 44.
4.5	29	Full time-domain response of hinge plate.
4.6	29	Frequency-domain representation of hinge plate time-domain results.
4.7	30	Time-domain representation of hinge plate solution highlighting the first mode, where the period $T = 0.0111$ second, whose reciprocal equals 89.82 Hz.

Fig.	Page	Caption
4.8	31	Time-domain representation of hinge plate solution highlighting the second mode, where the period $T = 0.004$ second, whose reciprocal equals 243.53 Hz.
4.9	31	Time-domain representation of hinge plate solution highlighting the third mode, where the period $T = 0.00176$ second, whose reciprocal equals 568.16 Hz.
4.10	32	Graphical representation of the viscous damping function for the frequency-domain analysis of the hinge plate.
4.11	33	Forcing function for the frequency-domain analysis of the hinge plate.
4.12	34	Transformed frequency-domain representation with $\Delta f = 0.2$ Hz and frequency range = 9000 Hz, compared to Femap time-domain representation.
4.13	35	Transformed frequency-domain representation with $\Delta f = 0.6666$ Hz and frequency range = 9000 Hz, compared to Femap time-domain representation.
4.14	35	Transformed frequency-domain representation with $\Delta f = 1.3333$ Hz and frequency range = 9000 Hz, compared to Femap time-domain representation.
4.15	36	Frequency-domain comparison between frequency-domain data at $\Delta f = 0.6666$ Hz and transformed time-domain data.
4.16	37	Frequency-domain comparison between frequency-domain data at $\Delta f = 0.6666$ Hz and transformed time-domain data focused on the first mode.
4.17	37	Frequency-domain comparison between frequency-domain data at $\Delta f = 0.6666$ Hz and transformed time-domain data focused on the third mode.
4.18	38	Frequency-domain comparison between frequency-domain data at $\Delta f = 1.33333$ Hz and transformed time-domain data focused on the first mode.
4.19	39	Frequency-domain comparison between frequency-domain data at $\Delta f = 1.33333$ Hz and transformed time-domain data focused on the third mode.
5.1	41	Frequency-domain comparison between frequency-domain data at $\Delta f = 1.5$ Hz and transformed time-domain data focused on the first mode.

Fig.	Page	Caption
5.2	42	Transformed frequency-domain representation with $\Delta f = 1.5$ Hz and frequency range = 9000 Hz, compared to a time-domain solution in Femap.
5.3	45	Linear spectrum for the Femap output of the frequency-domain analysis with $\Delta f = 0.6666$ Hz.
5.4	46	Linear Spectrum of frequency-domain data with $\Delta f = 0.6666$ Hz, with Femap frequency sampled up to 1200 Hz.
5.5	46	Comparison of time signals computed with the original transformed spectrum and the reconstructed transformed spectrum.
5.6	49	Transformed frequency-domain representation with 100 Hz modal frequency and 12.5 Hz and 8.3333 Hz frequency resolutions, where extended periods = 0.08 seconds and 0.12 seconds.

List of Tables

Table	Page	Caption
4.1	25	Display of the 1 st 10 modes of vibration for the hinge model.
4.2	32	Values representing the viscous damping function for the frequency-domain analyses of the hinge plate.

Chapter 1. INTRODUCTION

Traditionally, structural-acoustic calculations are performed in the frequency-domain assuming time-harmonic or steady-state motion. Finite and boundary element methods have been studied extensively for these types of problems. However many important problems in engineering are inherently transient. For example, a purely frequency-domain analysis would be insufficient in modeling the initial startup of a rotating piece of machinery, where the spooling up of the rotating pieces in the machine excite natural resonances in the structure. But in general, time-domain calculations are less popular and haven't been developed to the same level of sophistication.

Boundary element computations, in particular, are almost always formulated in the frequency-domain. In these calculations, complex-valued matrices are generated representing transfer functions between the vibrations of the outer surface of a structure in contact with the acoustic medium and the resulting sound radiation. Many physical phenomena can be represented this way, but not in the time-domain where the equations of motion are written as purely real. An example of this would be a system with hysteretic damping, represented using a complex modulus, which has no time-domain equivalent.

While it would certainly be possible to derive transient boundary element computations from first principles, it would be much more computationally efficient to use existing frequency-domain programs to derive a transient solution. The main goal of this thesis is to explore the possibility of using the Fast Fourier Transform (FFT) to produce accurate and efficient transient solutions for structural vibration problems. The extension of the results to structural-acoustic problems should be trivial, but is beyond the scope of this thesis.

In dealing with very large models, the time of analysis becomes a primary concern. It is desirable to produce the most accurate solution in the least amount of time. Aside from proving that an accurate solution can be obtained, a secondary goal is to develop general guidelines for how to choose analysis parameters such as the upper analysis frequency and frequency spacing for the frequency-domain calculations, and the sample rate and overall analysis time for transient calculations. These guidelines will be

developed by comparing transient solutions calculated using transform techniques with analytical or numerical solutions that are known to be accurate.

Initially, a simple one degree-of-freedom spring mass system will be used as a test case to catalog solution accuracy as a function of frequency range and resolution. The spring mass system will be modeled and analyzed using Femap w/NX NASTRAN.¹ The system will be modeled with viscous damping for two different values of damping. One value represents a relatively low level of damping and the other represents a relatively high level. Two values were chosen to provide two concurrent sets of data, and are not meant to be representative of real-world engineering problems. The resulting frequency-domain data will be transformed to the time-domain and then compared to time-domain data known to be accurate. Certain general conclusions will be made based on the correlation between the two sets of data. These conclusions will form the basis for a set of parameters dictating the fastest and most efficient computational techniques for transient acoustic field calculations. The appropriate tradeoff between accuracy and computation time for the given method will be highlighted.

To verify the guidelines developed for the simple spring mass system, the same approach utilized for the simple spring mass system will be applied to a more general finite element problem of a hinge plate. Additional guidelines are necessary for this problem because it has multiple resonances, each with a different damping level. The results will show that the frequency spacing must be chosen to resolve the sharpest peak and the sample rate must be chosen to adequately resolve the highest frequency of interest. Fundamentally, these results are expected. A cursory examination would lead one to believe that transform techniques would be very inefficient due to the frequency range required to produce the desired sample rate in the time-domain. However, it will be shown that “zero-padding” and interpolation can be used to reduce the overall computation times.

In general, the basic techniques for transforming between the time- and frequency-domains are well known. However, there are relatively few references available on the subject of performing transient numerical calculations using Fourier transform techniques. The book by Nashif et al.² is primarily concerned with damping, but it does have a relatively complete discussion of Fourier transform techniques for

single degree of freedom systems. There have been several recent papers on the subject including Martins et al.,³ Barkanov et al.,⁴ Akay et al.⁵ and Mehl and Miles.⁶ Also, the computer code NASTRAN¹ by McNeil-Schwindler has the capability to perform transient analyses using Fourier transform techniques. Thus, the general ideas discussed in this thesis are not original. However, none of the references give an exhaustive list of guidelines for accurate transient computations, which is the goal of this thesis.

Chapter 2. BASICS OF THE ANALYSIS METHOD

Time-Domain Analyses

In order to determine the accuracy of a frequency-domain solution transformed into the time-domain, it is necessary to have an accurate time-domain solution to which the transformed solution can be compared. The finite element analysis program NASTRAN can be used to produce accurate time-domain solutions with its “direct transient” solution sequence for general problems. The method used is implicit and is similar to the Newmark Method as described by Bathe.⁷ According to Blakey,⁸ the structural response is computed by solving a coupled set of equations using direct numerical integration. The structural response is solved at discrete times, the velocity and acceleration are represented using a central finite difference, and the applied force is averaged over three adjacent time points. The solution behaves like a succession of static solutions with each time step performing a forward-backward substitution on a new load vector. To test the accuracy of NASTRAN’s solver, a simple one degree-of-freedom spring mass system can be solved analytically for the time-domain response. Then, the same one degree-of-freedom spring mass system can be modeled and solved using Femap w/NX NASTRAN. If these two solutions match, a conclusion can be made about whether or not NASTRAN’s “direct transient” solver produces an accurate time-domain solution for comparison purposes.

The first step in making a comparison is to generate an analytical time-domain solution for a simple one degree-of-freedom spring mass system where a force F is applied to the mass. The equation needed to do this is described by Nashif et al.²

$$\frac{w(t)}{F} = \frac{1}{\pi} \int_0^\infty \frac{[(k-m\omega^2) \cos \omega t + k\eta \sin \omega t]}{(k-m\omega^2)^2 + (k\eta)^2} d\omega, \quad \text{Eq. (2.1)}$$

where k is spring stiffness, m is mass, t is time, η is loss factor, ω is the natural frequency and variable of integration and $w(t)$ is the displacement of the mass. Because viscous damping will be specified, it would also be possible to write the solution in analytical form. However, the solution derived using Fourier transform techniques is used instead to keep the same format as in the discussion given by Nashif et al.² If this integration is

performed for a number of values of t , the result is the time-domain response of the spring mass system to a perfect unit impulse. In the real world, such an impulse could be generated by striking the system at a selected point with a hammer.

For the purpose of demonstration, Equation 2.1 is solved using Matlab's⁹ *quad* command for a case with viscous damping where the spring stiffness k is constant with frequency and η increases linearly with frequency. Matlab loops over a range of t and the other variables are set as follows:

$k = 2910 \text{ N/m}$
 $m = 0.0073711 \text{ kg}$
 $\eta = (2.28 \times 10^{-4}) * \omega$
 $\infty = 10^5$ (need a value here so Matlab can perform the integration numerically)

The loss factor η is set to match the parameters of an analytical solution presented in Nashif et al.² Again, it would be possible to specify a viscous damping coefficient directly, but loss factors are specified instead to maintain the same format as Nashif et al.² The spring value k and the mass value m selected set the modal frequency f of the system to a convenient and straightforward value of 100 Hz,

$$f = \frac{1}{2\pi} \sqrt{\frac{k}{m}} . \quad \text{Eq. (2.2)}$$

The response of the system calculated by Matlab is displayed in Figure 2.1:

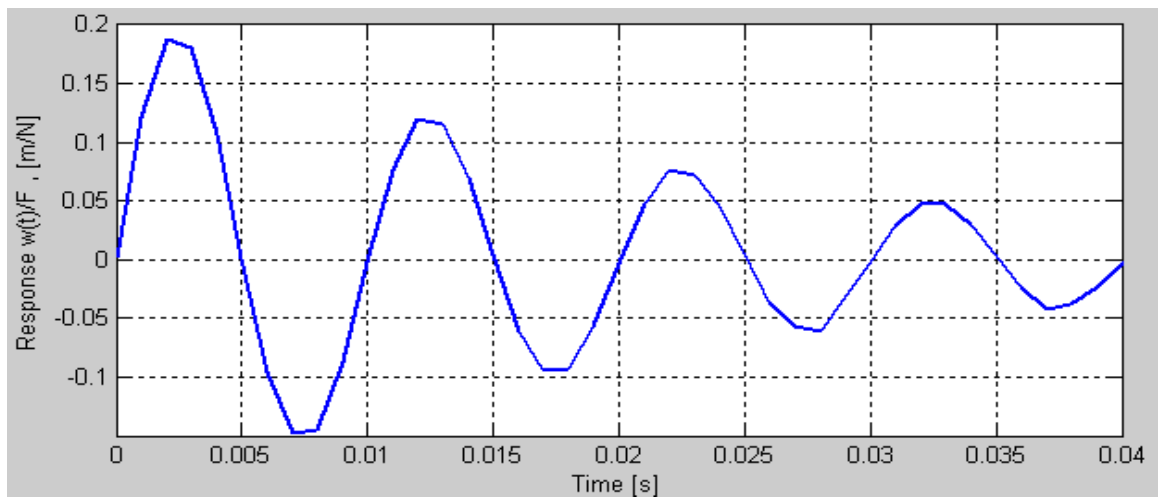


Figure 2.1. The first 0.04 seconds of the analytical solution for the damped spring mass system as calculated by Matlab.

The next step in the process is to model the spring mass system in Femap. The system can be modeled with two nodes, connected by a spring. The node on the left is fully fixed in all translational and rotational directions. The node on the right represents a mass property and is fixed in all directions except for the translational x-axis.

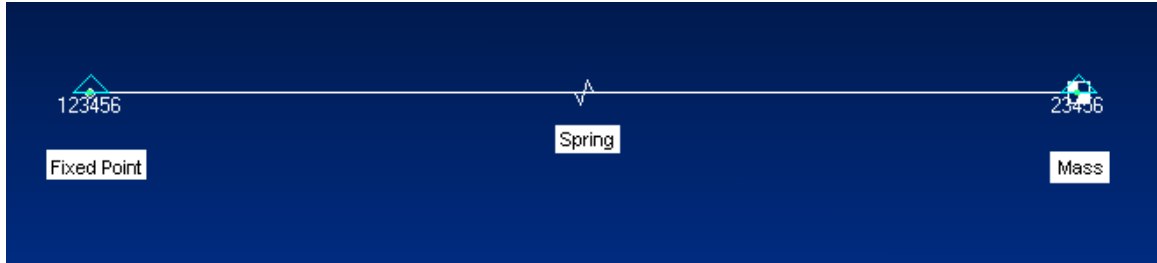


Figure 2.2. Femap model of the spring mass system, a fixed point and a mass connected by a spring property.

To analyze this model in the time-domain, we need to apply a time-domain impulse forcing function to the mass in the x direction. Unfortunately Femap doesn't allow us to create a perfect impulse and apply it to the system. Instead, an impulse will be constructed that starts at a value of zero, rises to a value of one, and returns to a value of zero fast enough that it represents a pure impulse without creating a visible starting transient or "ramp-up" on a plot of the time-domain solution. The values used to create this impulse are shown in Figure 2.3.

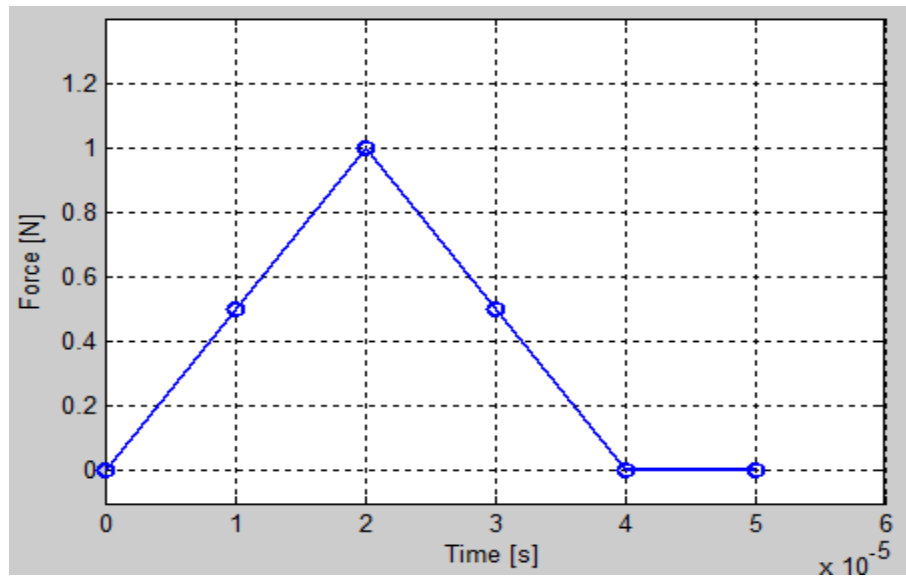


Figure 2.3. Graphical representation of the time-domain forcing function used in Femap.

It is also important to set the variables in Femap to match those used in the analytical solution. The mass property for the node on the right is set to $m = 0.0073711$ kg, and the spring property connecting the two nodes is set to $k = 2910$ N/m. As described in Blakely,⁸ for Femap's "direct transient" analysis, the only damping condition available is viscous damping where the resulting forces are proportional to velocity. Most real world applications have damping more closely characterized as hysteretic, where the damping forces are proportional to displacement and are typically modeled using a complex stiffness as discussed by Nashif et al.² However, since the key to verifying the validity of the guidelines presented in this thesis rests on comparing transformed frequency-domain data to accurate time-domain data, a real-valued viscous damping condition must be used for all example analyses. The example viscous damping condition is created by assigning values for two parameters, "equivalent viscous damping" and "frequency for system damping." Based on the values input, Femap creates a damping function that starts at zero and grows linearly up to the "equivalent viscous damping" value set at the "frequency for system damping." In other words, a viscous damping condition is created that passes through the specified damping value for a specified frequency. To make sure the modal frequency of 100 Hz is captured, the frequency for system damping is set to 200 Hz and the damping η at this point is calculated based on:

$$\eta = 2.28 * 10^{-4} * 2\pi f , \quad \text{Eq. (2.3)}$$

as introduced earlier on page 4 as a frequency dependent viscous damping condition. This process ensures that the damping at 100 Hz matches the damping for the analytical solution. Using Equation 2.3, the result is $\eta = 0.2865$ at 200 Hz, and this value is input as "equivalent viscous damping" in Femap. According to the viscous damping condition, this sets the damping to $\eta = 0.14325$ at our 100 Hz frequency of interest.

Since this is a very simple system, it allows us to produce a very accurate and well resolved time-domain solution in a very short amount of time using Femap's "direct transient" solver. The sample frequency for this time domain analysis is 10,000 Hz, so the response or physical displacement of the system to the impulse is being sampled

every 0.0001 second, for 1500 samples. The response is plotted in Figure 2.4, and the NASTRAN input deck for this analysis is located in Appendix C.

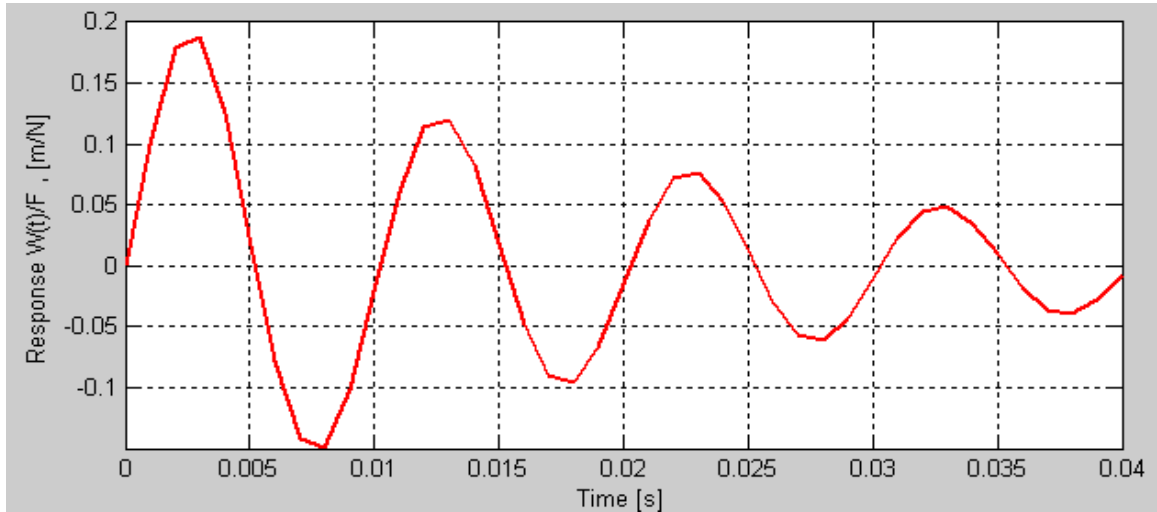


Figure 2.4. Femap time-domain analysis of spring mass system previously calculated analytically in Figure 2.1.

Figure 2.5 shows, a comparison between the analytical solution and NASTRAN's “direct transient” solution:

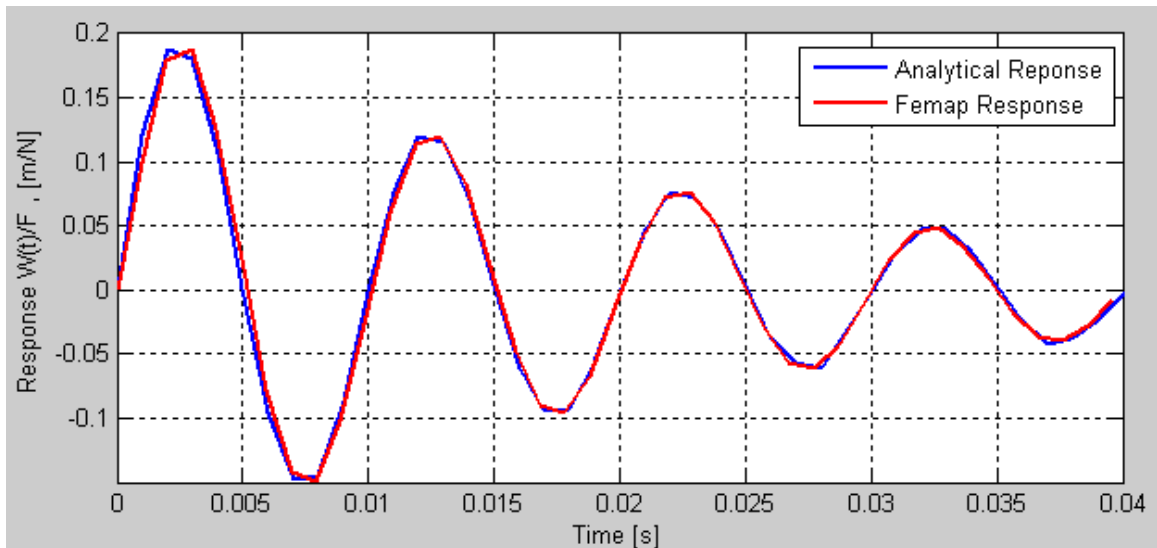


Figure 2.5. Comparison plot of the analytical response to the Femap response of the same system.

A visual inspection of Figure 2.5 indicates that NASTRAN's “direct transient” solver produces a very acceptable time-domain solution for the simple spring mass

system response to an impulse. Any differences can most likely be attributed to Matlab's finite approximation for the infinite upper limit of the integral. This is a good indication that for more complicated systems, NASTRAN's "direct transient" solution can be trusted as an accurate solution for which transformed frequency-domain data can be compared.

Frequency-Domain Analyses

The frequency-domain analyses performed using Femap w/NX NASTRAN produce the data to be transformed to the time-domain. Continuing on with the example of the spring mass system with a resonance at 100 Hz, the first step is again to set the physical properties of the system. The mass property of the node on the right is set to $m = 0.0073711$ kg, and the spring property connecting the two nodes is set to $k = 2910$ N/m. For NASTRAN's "modal frequency" solver, the damping is set using a "modal damping table," where a "structural damping" function must be specified. To match the viscous damping specified for the previous time-domain example analysis, the damping function is formed point by point and is shown in Figure 2.6. Again, the damping value at our 100 Hz frequency of interest is $\eta = 0.14325$.

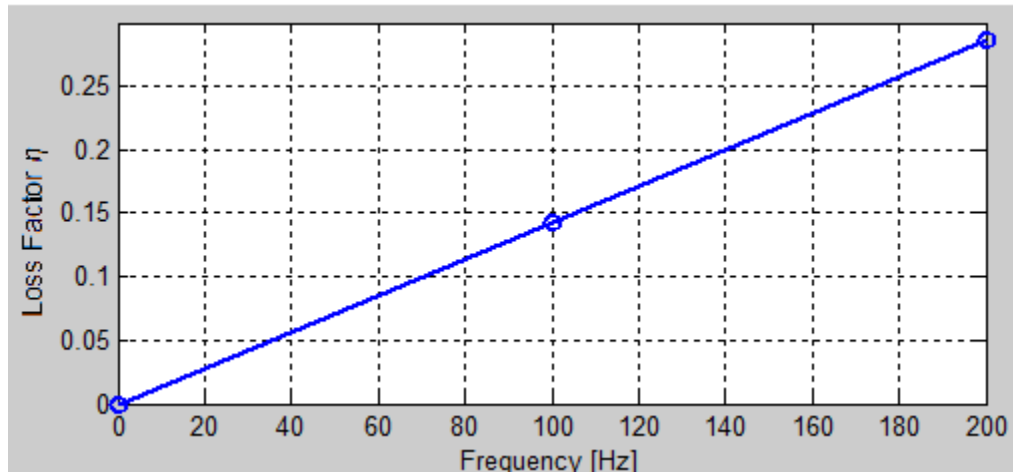


Figure 2.6. Viscous damping function for Femap frequency-domain analysis of a spring mass system.

Applying an impulsive force to the system in the frequency-domain is actually quite simple. Since a pure impulse transformed into the frequency-domain is a consistent flat response across all frequencies, we need to simply create a frequency forcing

function to match this. To capture the 100 Hz modal frequency of interest, the system will be forced with a flat frequency response force of 1 N from 0 Hz to 200 Hz, as illustrated in Figure 2.7.

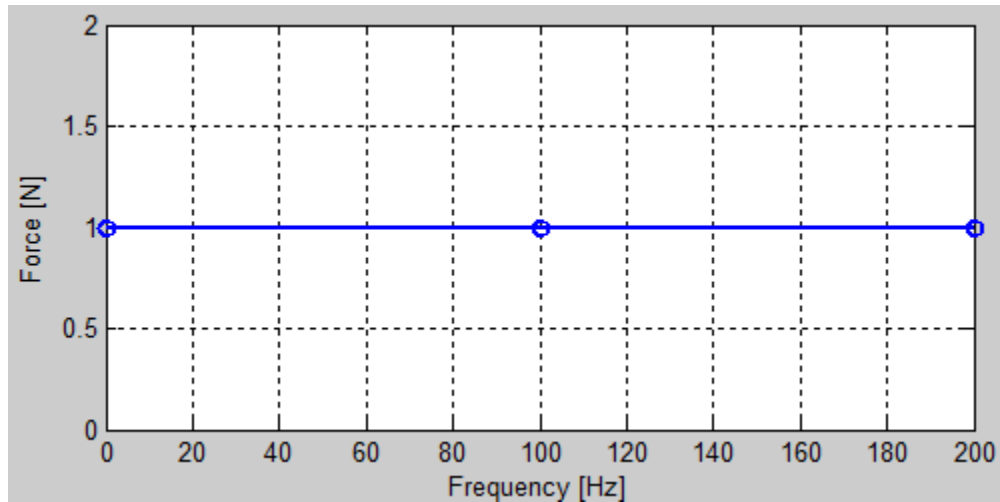


Figure 2.7. Forcing function for Femap frequency-domain analysis of a spring mass system.

Once the physical system properties are selected and the forcing function is established, one can proceed with NASTRAN’s “modal frequency” analysis. The two parameters that are specified as part of this analysis are frequency range and frequency resolution. Frequency range is how high the frequency analysis will go, and the frequency resolution is how often along the frequency axis the response is sampled. Setting these two parameters is very important since the lower they are set, the faster the computation will be.

The data from the modal frequency response analysis is complex-valued. It’s important to note that this analysis cannot produce values at zero frequency, so these values must be interpolated and set before manipulating the data.

Preparing the Data for Comparative Analysis

Unfortunately, the raw data exported from Femap isn’t scaled for a unit impulse. Similar to a Dirac Delta function, the amplitude of the impulse is related to the area under a curve of input force versus time. Figure 2.3 is repeated as Figure 2.8 for convenience:

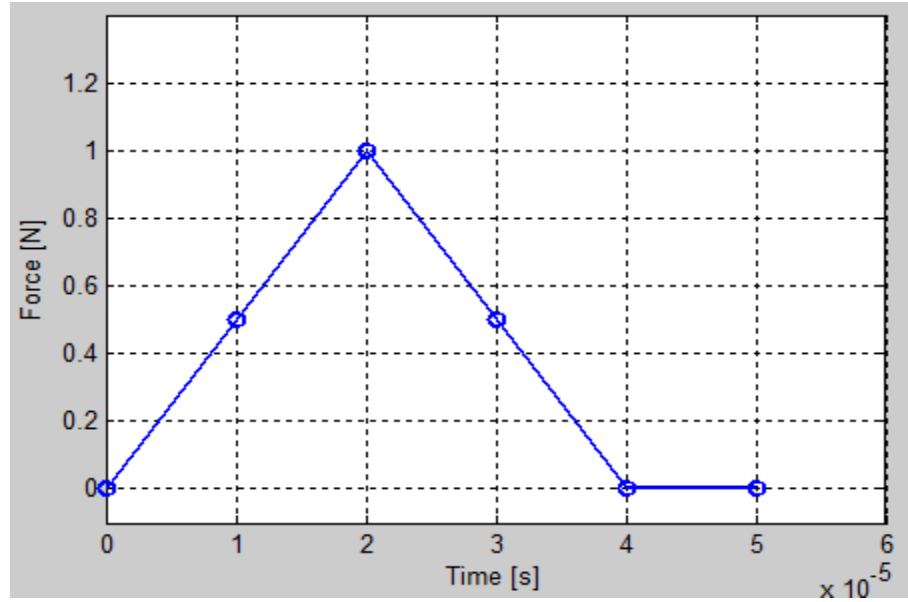


Figure 2.8. Graphical representation of the time-domain forcing function used in Femap.

In Figure 2.8, which is a plot of the time-domain forcing function, the area under the curve equals 0.00002 Ns. Therefore, it is necessary to multiply the time-domain response data by 0.00002^{-1} , or 50,000 to accurately represent the response of the system to a unit impulse.

For the frequency-domain, the real and imaginary components for each frequency point must be combined together into a complex number, that is: $\text{real} + i \cdot \text{imaginary}$. Then, in order to form a full linear spectrum that goes from 0 Hz to the sample frequency f_s in the time-domain after transformation, one must take all of the complex points excluding the zero frequency point and the $f_s/2$ frequency point, mirror them about the x-axis, take the complex conjugate and tag the new series onto the end of the original series. This process is illustrated by Gabrielson¹⁰ and is displayed in Figure 2.9.

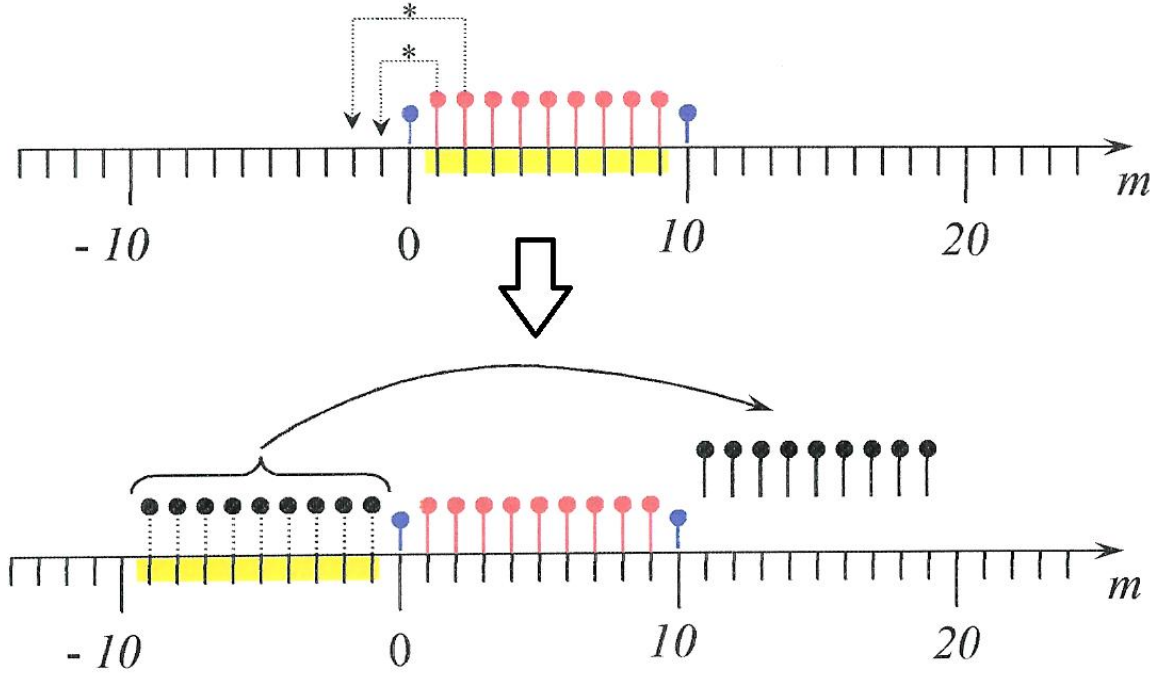


Figure 2.9. Graphical representation of taking the complex conjugate of frequency data, mirroring it across the x-axis, and then tagging the new series onto the end of the original data series, thus forming the full linear spectrum.

In addition, the zero and $f_s/2$ frequency points must be completely real, so the imaginary component of those points are forced to be zero. This produces a time-domain signal that is entirely real.

The linear spectrum is now ready to be transformed. The inverse Fourier transform (*ifft* command in Matlab) of the full spectrum is taken. The result should be a completely real time-domain representation, but will often include a small residual imaginary component ($\sim 1 \times 10^{-11}$) which can be ignored. According to Matlab's help files, the Matlab *ifft* command includes a factor that divides the set of data by the number of data points, $(1/N)$:⁹

$$x(j) = \left(\frac{1}{N}\right) \sum_{k=1}^N X(k) \omega_N^{-(j-1)(k-1)}. \quad \text{Eq. (2.4)}$$

So, the transformed data must be multiplied by the number of data points N . Lastly, to complete the data preparation, the inverse Discrete Fourier Transform as

described by Gabrielson¹⁰ requires that the data must also be multiplied by Δf , or the frequency resolution selected in Femap:

$$x_n = \sum_{m=0}^{N-1} X_m e^{j2\pi \frac{nm}{N}} (\Delta f) . \quad \text{Eq. (2.5)}$$

Once all of those conditions are met, the transformed frequency data is ready to be compared to time-domain data obtained using NASTRAN's "direct transient" solution sequence.

Before beginning to analyze actual problems, a brief discussion will be given of a somewhat unexpected difficulty that can occur if the system damping is not physically-realizable. In a real system, the damping must go to zero at zero frequency. However, it is possible to violate this requirement in a numerical calculation, especially when the damping is represented as being hysteretic. For example, it is common to assume the damping is proportional to stiffness and constant with frequency. In this situation, the computations may exhibit a non-causal response, such that the system will be displaced before an impulse is applied. This effect is documented by Nashif et al.² In general, this difficulty does not occur unless the damping is relatively large, so a non-causal response is unlikely for practical problems with realistic damping levels.

Chapter 3. SPRING MASS SYSTEM ANALYSIS

One of the primary parameters for a structural vibration problem is the upper frequency for the frequency-domain analyses. For example, a frequency-domain analysis in Femap including frequencies up to 500 Hz will fill out to 1000 Hz after the real and imaginary Femap output vectors are manipulated to include the full linear spectrum. That is, the frequency-domain representation of the response will include frequencies up to 1000 Hz. This frequency range of 1000 Hz translates to the sample frequency f_s in the time-domain after an inverse Fourier transformation. So in this example, once the frequency data is transformed to the time-domain, the Δt , or time spacing between points would be 0.001 second, or the inverse of the sample frequency f_s .

This frequency range parameter is very important because it determines the number of points per wavelength once the data is transformed to the time-domain. The frequency range must be selected so there are enough points to accurately display the time-domain waveform, but not so many points such that the level of detail is unnecessary. The Figures 3.1, 3.2 and 3.3 illustrate the effect of varying the frequency range, and have frequency ranges of 1000 Hz, 2000 Hz, and 1600 Hz respectively.

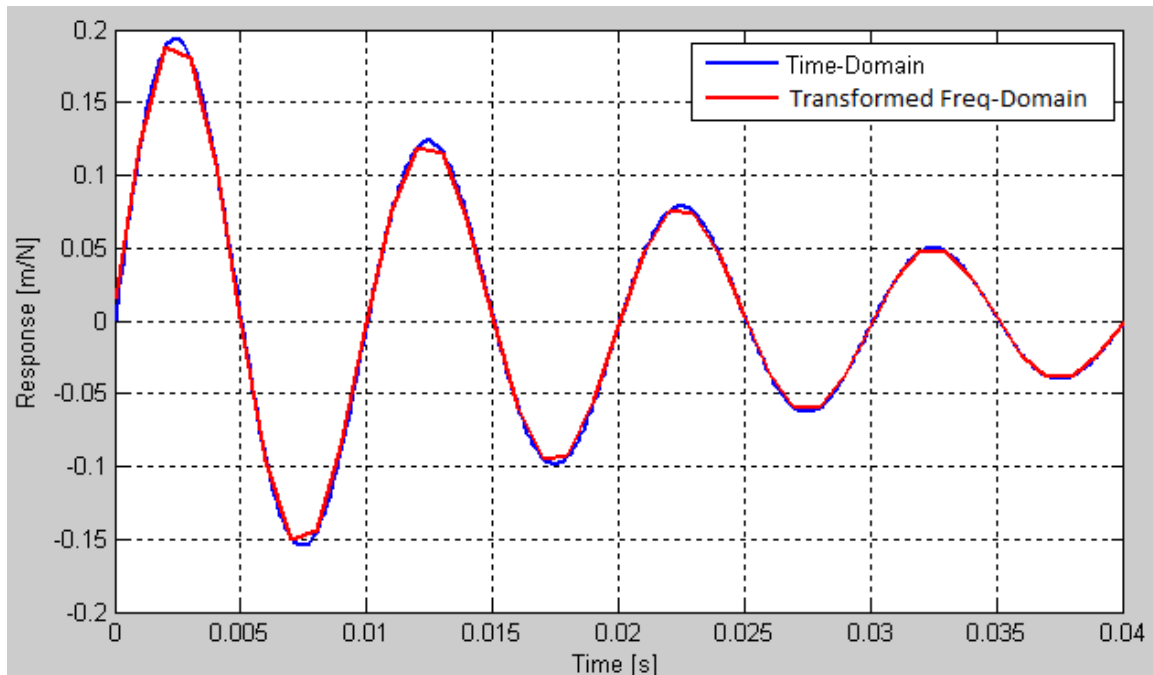


Figure 3.1. Transformed frequency-domain representation with 1000 Hz frequency range and modal frequency of 100 Hz, compared to Femap time-domain representation.

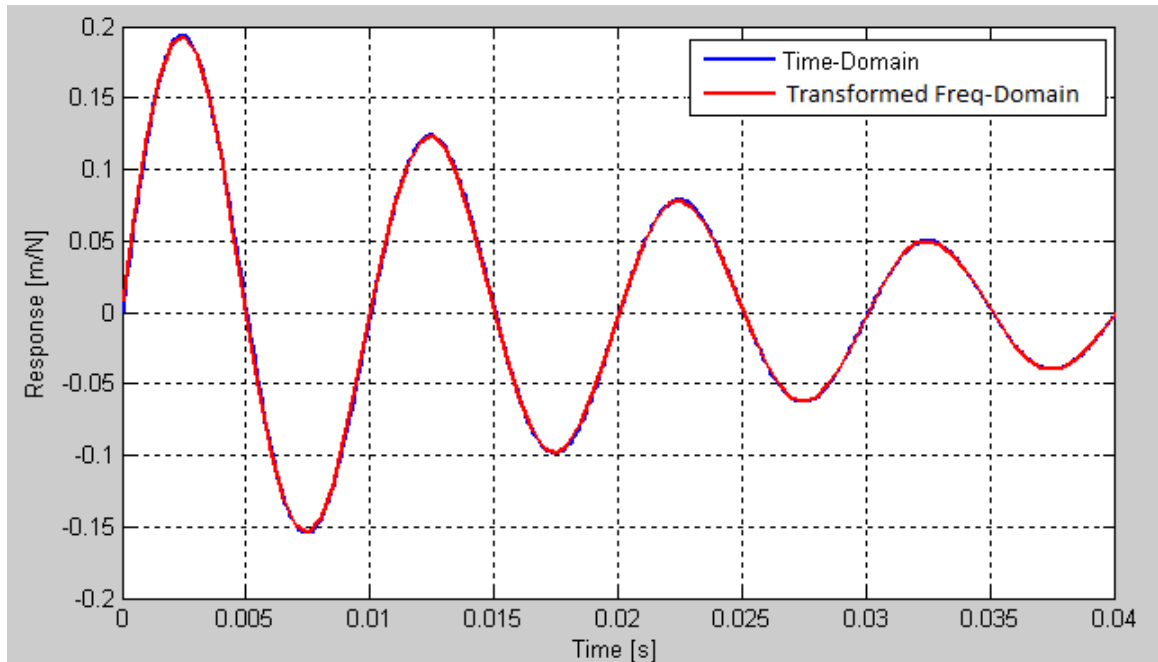


Figure 3.2. Transformed frequency-domain representation with 2000 Hz frequency range and modal frequency of 100 Hz, compared to Femap time-domain representation.

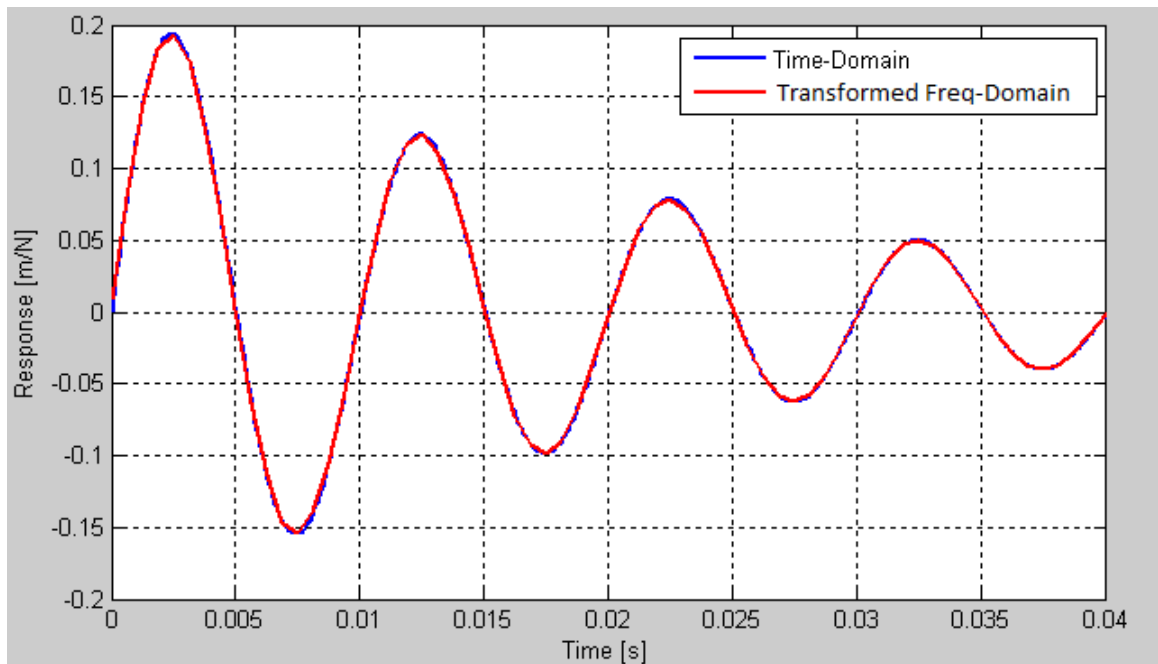


Figure 3.3. Transformed frequency-domain representation with 1600 Hz frequency range and modal frequency of 100 Hz, compared to Femap time-domain representation.

Figure 3.1 displays a frequency range that corresponds to 10 time steps per wavelength. It's clear that the amplitude is clipped and the transformed data is not a very accurate representation of the time-domain response. Figure 3.2 displays a frequency range that corresponds to 20 time steps per wavelength. The correlation between the two curves is very good, but the peaks are a little more resolved than necessary, leading to extra computation time. Figure 3.3 displays a frequency range that corresponds to 16 time steps per wavelength. This selection seems to be a fairly good compromise between the 10 and 20 point plots, with the even number of 16 being chosen because as an even number, 16 points can be spread evenly between the positive and negative halves of the waveform.

Of course, the overall accuracy looks different depending on the frequency range shown in the plot. Narrowing the frequency range tends to highlight differences between the curves. Roughly 16 time steps per wavelength seems to be a fairly good compromise between computation time and accuracy at reasonable zoom levels. Four points per quarter-wavelength should be enough in most cases to form the roughly semi-circular-shaped function. The validity of this compromise however is almost purely a matter of interpretation, as different projects may warrant different accuracy based on the scope and goals of the project. This 16 time steps per wavelength rule should therefore be treated more as a suggestive guideline rather than a hard rule.

Aside from frequency range, frequency resolution is another important parameter that can be altered to change the computation time in a frequency-domain analysis. Frequency resolution refers to the spacing in Hz between sample points in the frequency-domain. Obviously, the smaller the spacing, the more accurate the representation of the true frequency curve, but the greater the computation time.

In the best case scenario, the mode or modes of the system would fall directly at frequencies that are being sampled. For example, if the frequency resolution is 10 Hz and the modal frequency is 100 Hz, the peak of the mode will fall directly on a sample point. This scenario gives the best chance of producing an accurate time domain representation. However, in most systems, it is unlikely that all the modes will fall directly on sample points. The peak values will end up being at some degree between the sample points, with a worst case scenario of the mode falling directly in between two

sample points. Considering the 10 Hz frequency resolution example again, if the mode of the system ends up being 95 Hz instead of 100 Hz, the peak amplitude of the mode will fall directly in between the sample points at 90 Hz and 100 Hz. In this scenario, as opposed to the on-bin scenario, for the same frequency resolution, there is less of a chance that the time-domain data will reflect the true amplitude of the response.

The on-bin and off-bin scenarios actually produce two opposing amplitude results as frequency resolution degrades. As the spacing between sample frequencies increases, the off-bin case produces amplitudes too low in the time-domain since the peak amplitude of the mode in the frequency-domain is cut off. At the frequency resolution where this amplitude decrease starts to occur, an on-bin scenario will often still produce a good result. But as frequency spacing increases, the on-bin case starts to produce amplitudes that are too high since the peak amplitude is captured in the frequency-domain, but the sides of the peak start to broaden out and produce higher overall amplitudes across the frequency band near the resonance.

Therefore, an on-bin mode will generally produce better results than an off-bin mode, but since large models will usually have many resonance frequencies, the analysis of an unknown system should be planned according to the worst case scenario. The safe assumption is that every mode will fall exactly in between two frequency sample points. The selection of frequency resolution according to this plan will ensure an accurate time-domain response is computed.

The method that will be tested for selecting an appropriate frequency resolution involves the modal frequency f of the system, the frequency resolution Δf , and the loss factor η . The amount of damping at a particular frequency determines the width of that frequency peak in a frequency-domain representation. Therefore, the selected frequency resolution must depend on the modal frequency and the damping. Generally speaking, in order to get a somewhat accurate time-domain representation of the response, it's good practice to adhere to the following rule:

$$\Delta f < \eta * f , \quad \text{Eq. (3.1)}$$

where the frequency resolution selected should be less than the product of the modal frequency and the damping at that frequency. A response curve is a quadratic function near its peak, and three points are required to define a quadratic function. When the peak is sampled at its maximum value, the neighboring samples are at the 3 dB down points if $\Delta f = 0.5\eta*f$. The results presented in Figures 3.4 – 3.9 will show that it is permissible to relax this requirement slightly and follow Equation 3.1 instead. The relationship proposed in Equation 3.1 will be tested using three separate plots for two different damping values. The first plots shown in Figures 3.4 and 3.7 display scenarios where the frequency resolution is much less than the product of the modal frequency and the damping. The middle plots shown in Figures 3.5 and 3.8 display scenarios where the frequency resolution and the product of the modal frequency and the damping are nearly equal. The final plots shown in Figures 3.6 and 3.9 display scenarios where the frequency resolution is much greater than the product of the modal frequency and damping. All plots have a frequency range of 1600 Hz, so that there are roughly 16 points per wavelength for each plot.

Figures 3.4-3.6 show plots for viscous damping = 0.2865 at 200 Hz.

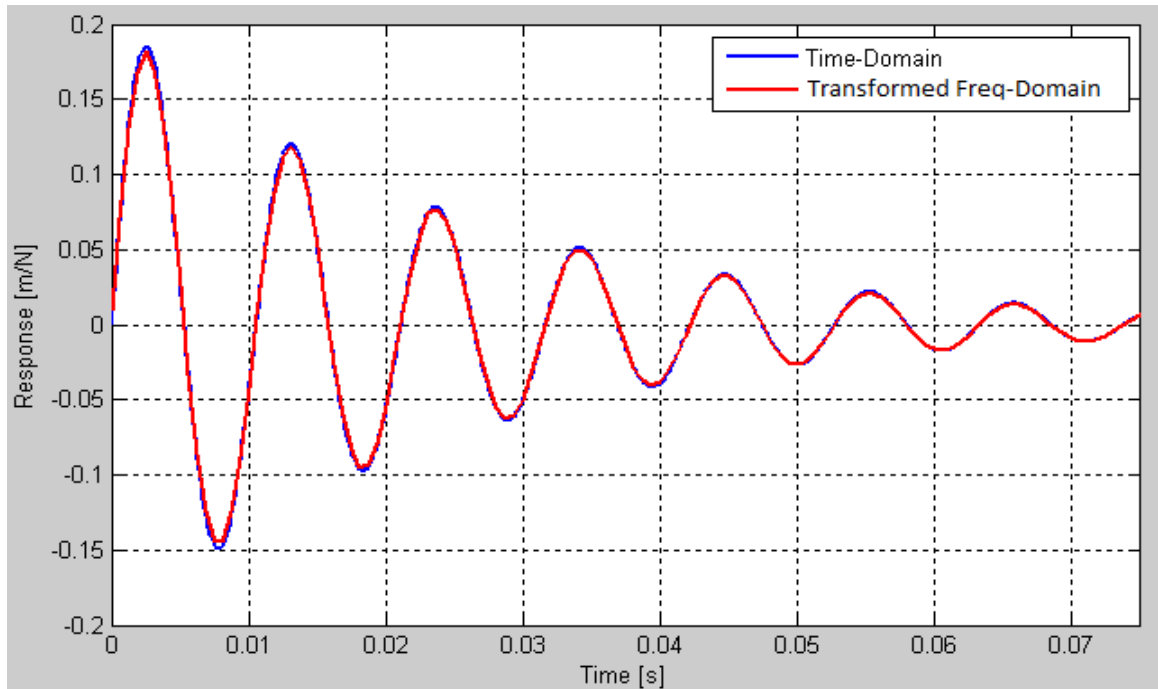


Figure 3.4. Transformed frequency-domain representation with 95 Hz modal frequency, 1600 Hz frequency range and 10 Hz frequency resolution, compared to Femap time-domain representation.

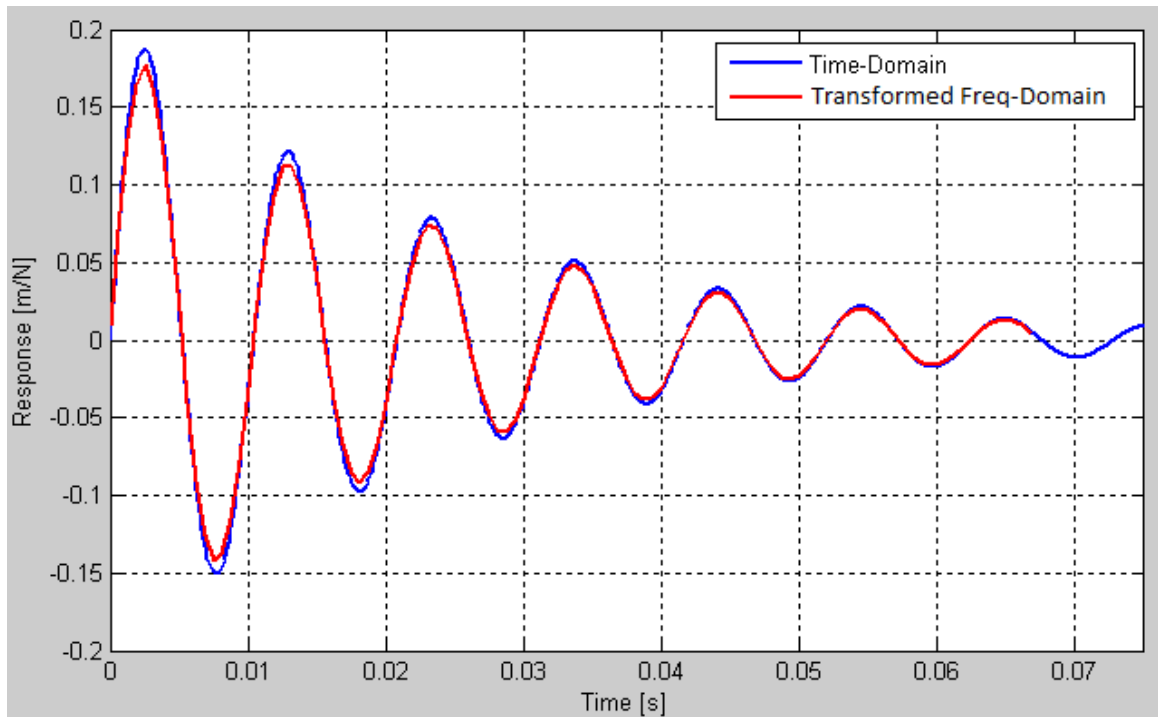


Figure 3.5. Transformed frequency-domain representation with 96.3 Hz modal frequency, 1600 Hz frequency range and 14.8 Hz frequency resolution, compared to Femap time-domain representation.

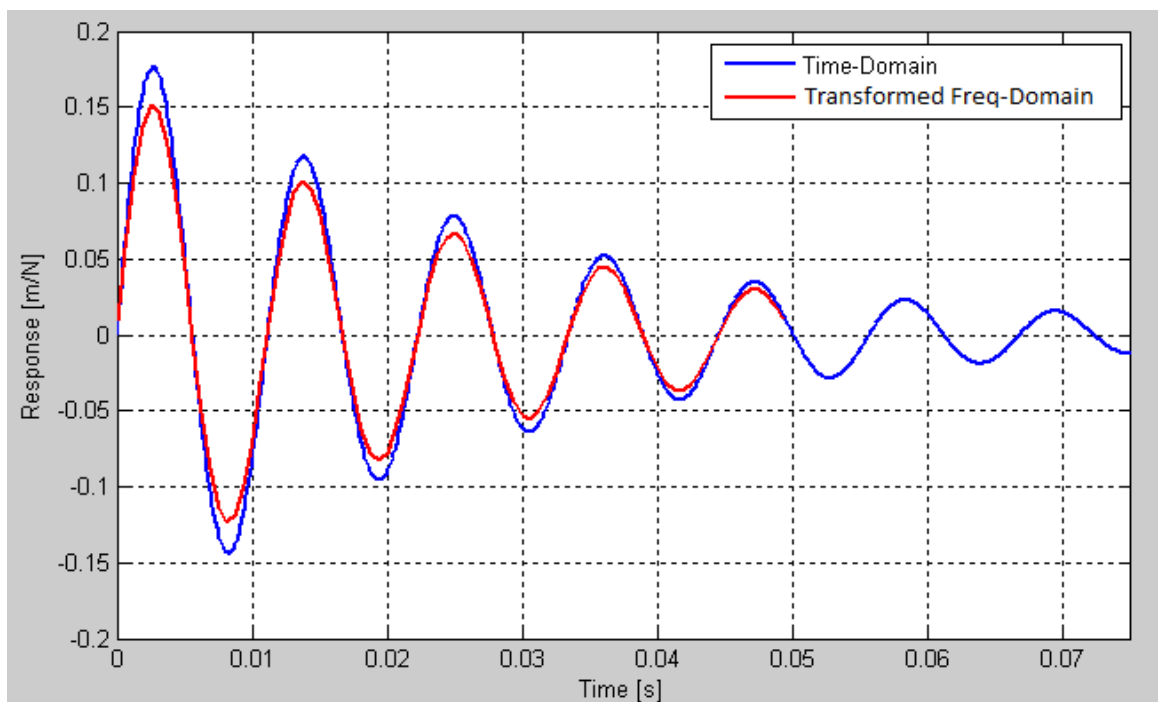


Figure 3.6. Transformed frequency-domain representation with 90 Hz modal frequency, 1600 Hz frequency range and 20 Hz frequency resolution, compared to Femap time-domain representation.

In Figure 3.4, $\Delta f = 10$ Hz and $\eta^*f = 12.93$. Since Δf is less than η^*f , the two curves match up very well. In Figure 3.5, $\Delta f = 14.8$ Hz and $\eta^*f = 13.29$. Since Δf is slightly larger than η^*f , the amplitude of the transformed data is starting to fall in relation to Femap's time-domain data. In Figure 3.6, $\Delta f = 20$ and $\eta^*f = 11.6$. Since Δf is well above η^*f , the two curves are clearly very different.

Figures 3.7-3.9 show plots for viscous damping = 0.12 at 200 Hz.

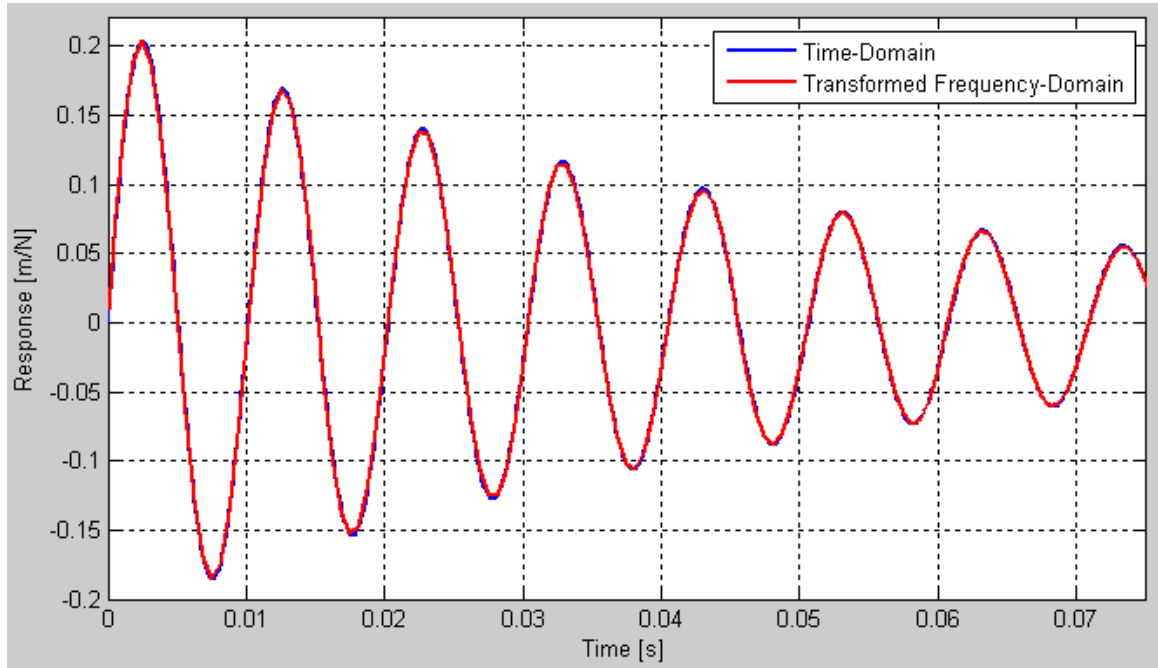


Figure 3.7. Transformed frequency-domain representation with 98.75 Hz modal frequency, 1600 Hz frequency range and 2.5 Hz frequency resolution, compared to Femap time-domain representation.

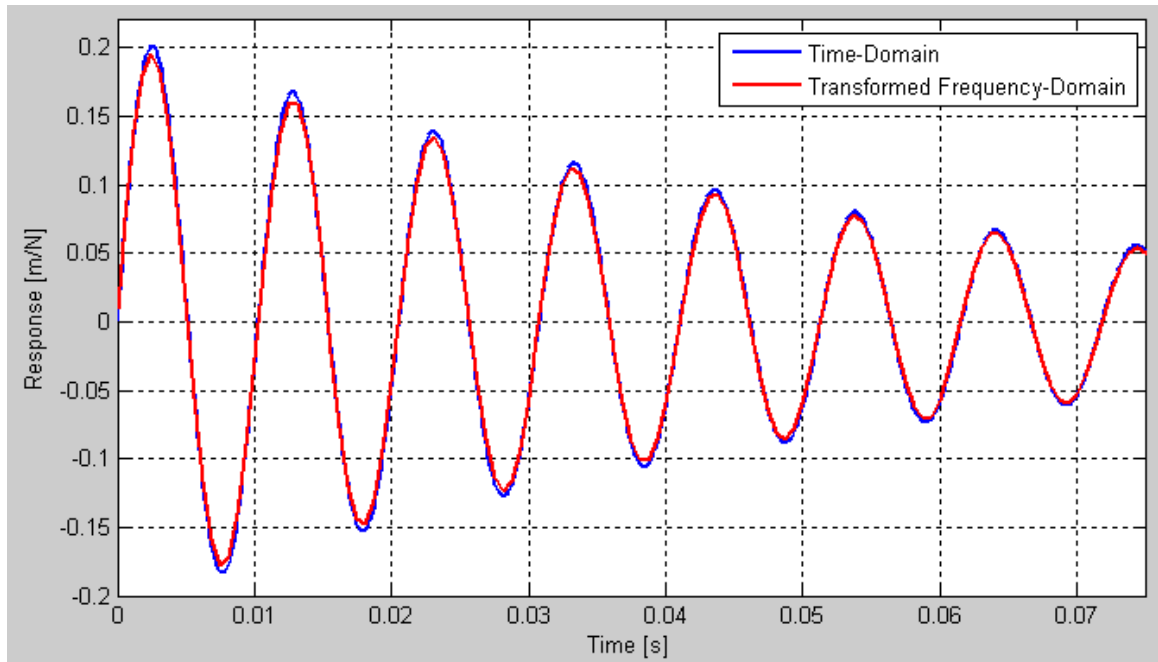


Figure 3.8. Transformed frequency-domain representation with 97.5 Hz modal frequency, 1600 Hz frequency range and 5 Hz frequency resolution, compared to Femap time-domain representation.

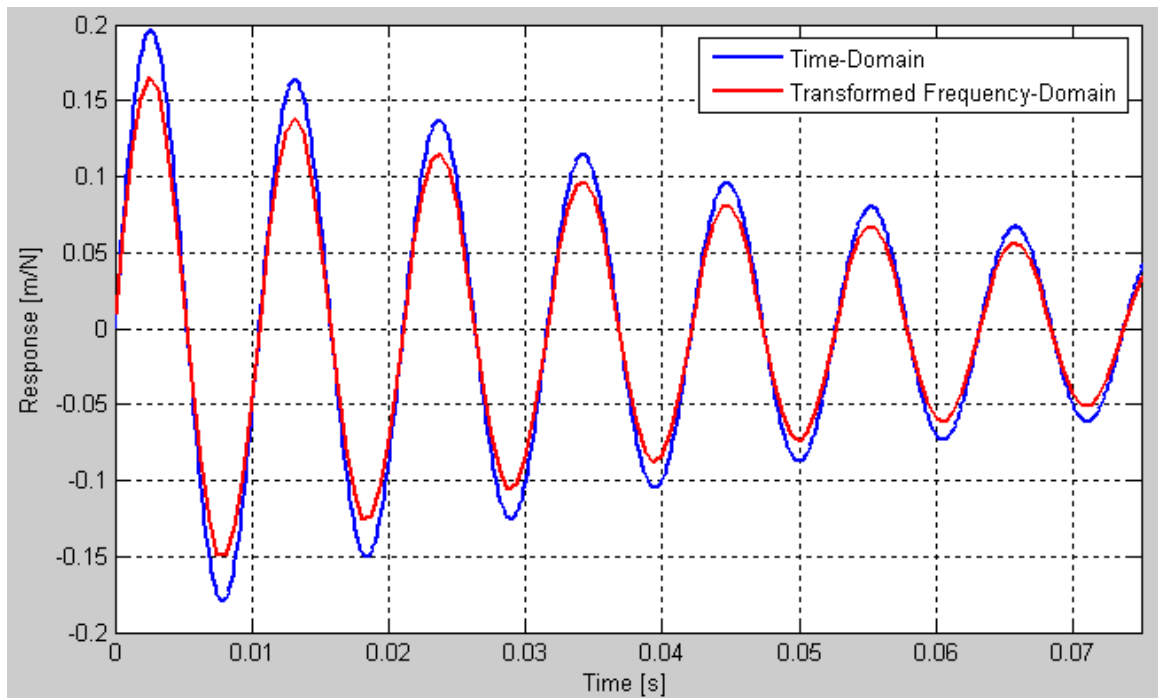


Figure 3.9. Transformed frequency-domain representation with 95 Hz modal frequency, 1600 Hz frequency range and 10 Hz frequency resolution, compared to Femap time-domain representation.

In Figure 3.7, $\Delta f = 2.5$ Hz and $\eta^*f = 5.85$. Since Δf is less than η^*f , the two curves match up very well. In Figure 3.8, $\Delta f = 5$ Hz and $\eta^*f = 5.7$. Since Δf has started to creep towards η^*f , the amplitude of the transformed data is starting to fall in relation to Femap's time-domain data. In Figure 3.9, $\Delta f = 10$ and $\eta^*f = 5.42$. Since Δf is well above η^*f , the two curves are clearly very different.

As a caveat to the above results, it is very important to be aware that frequency resolution Δf in the frequency-domain determines the overall length of the resulting time-domain waveform once it is transformed. For example, if a linear spectrum is sampled at $\Delta f = 5$ Hz, the resulting time-domain waveform will be 0.2 seconds long, or 1/5 of a second. It may be that the system is damped at such a level that the response falls to a marginal level before 0.2 seconds. But, if the system is not damped very much, a frequency resolution of 5 Hz in the frequency-domain may not be fine enough to capture the entire useful length of the time-domain response. Thus, it is important to keep in mind that trying to be too computationally streamlined with a large frequency resolution may result in lost data at the end of a time series. This issue is further discussed in Chapter 5.

The above results clearly show that adhering to the $\Delta f < \eta^*f$ rule can serve as a solid general guideline for these kinds of analyses. The point at which the two sides of this equation are equal does seem to be where serious degradation in amplitude of the time-domain response starts to take place. However, the degree of acceptable degradation is again subject to interpretation and varies depending on the scope and goals of individual projects. But, this relationship does serve as a reasonable starting point for selecting a frequency resolution that will yield an accurate result, but is still computationally efficient.

Now that this method has been tested on the simple one degree-of-freedom mass spring system, it can certainly be applied to larger system models which may contain many modes and interesting damping conditions across the frequency spectrum. From the results collected from our analysis of the simple spring mass system, it follows that the frequency range must be selected based on the highest mode of interest. For example, if there are three modes at 10 Hz, 50 Hz, and 100 Hz, the frequency range must be selected based on the 100 Hz mode. Selecting the frequency range to be 160 Hz will

allow the 10 Hz contribution to the time-domain response to have 16 points per wavelength, but the 100 Hz contribution will only have 1.6 points per wavelength, which is insufficient. Therefore, the frequency range must be selected based on the highest resonance frequency so that the contribution from that mode to the time-domain response is clearly and accurately resolved. And of course, the lower modes will be easily resolved by this high frequency range selection.

For large models with many modes, the frequency resolution selection will be determined by the damping of the system. If the system is viscously damped, where viscous damping effects on displacement increase linearly with frequency, the value of $\eta*f$ will increase as the modal frequencies increase and it is suggested that the frequency resolution must be selected to be less than the $\eta*f$ value of the lowest mode. The same rules apply when the damping is modeled as being hysteretic rather than viscous. If we have a constant damping value of $\eta = 0.15$, and there are modes at 50 Hz and 100 Hz, the width of the peak at 50 Hz will be smaller than the width of the peak at 100 Hz. So again, frequency resolution would be selected to be less than the $f*\eta$ value for the lowest frequency mode.

Chapter 4. ANALYSES FOR FINITE ELEMENT MODELS

Now that a general guidelines have been established based on a simple one degree-of-freedom spring mass system, the analysis will be extended to a more complex structure. The goal is to ensure the results from the simple one degree-of-freedom spring mass system apply to more complex structures, as well as exposing any other issues that may arise when analyzing a structure with more than one mode.

The structure chosen for the analysis is one of the example finite element models provided in the Femap software package. This particular structure was chosen because it contains multiple modes, but is still small enough that computation times are reasonable given limited available computational resources. The structure is described as a “hinge plate” made of $\frac{1}{4}$ ” thick AISI 4340 Steel, and has been modeled as 288 nodes with 240 elements, as illustrated in Figure 4.1. The nodes around the edge of the hole in the upper left portion of the hinge are constrained in all translational and rotational directions, while the rest of the nodes are free to move in all translational and rotational directions.

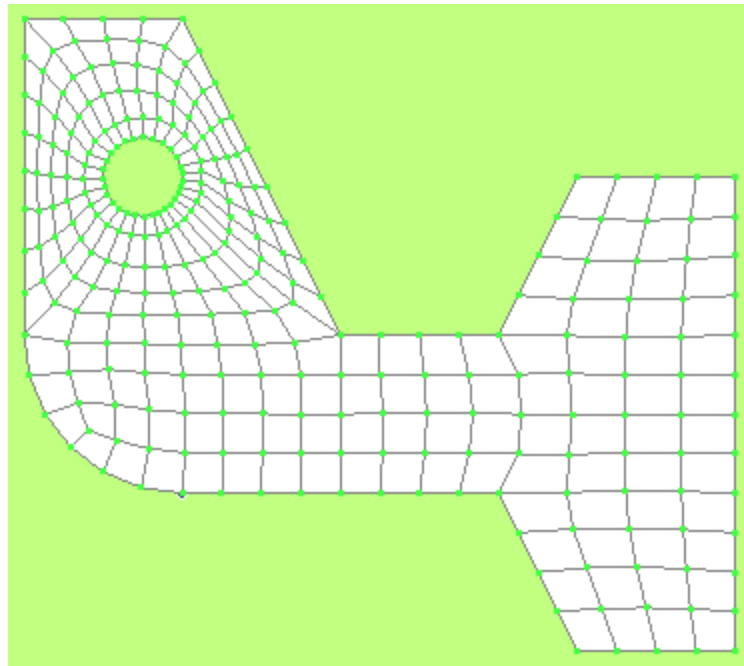


Figure 4.1. Femap “hinge plate” model, broken into 288 nodes with 240 elements.

The first step is to perform a NASTRAN “normal modes/eigenvalue” analysis. The resonance frequencies extracted from this analysis will then dictate the time-domain and frequency-domain analysis parameters. The resonance frequencies for the hinge plate are listed in Table 4.1.

Table 4.1. Display of the 1st 10 modes of vibration for the hinge model.

Mode Number	Frequency [Hz]
1	89.82
2	243.53
3	568.16
4	665.34
5	1012.37
6	1529.47
7	1986.73
8	2095.91
9	2102.15
10	2770.99

The subsequent analysis will focus on the 89.82 Hz, 243.53 Hz and 568.16 Hz modes to simplify the analysis and shorten computation times, yet it will still effectively highlight the intricacies involved with these types of analyses. Figure 4.2 displays the mode shapes of the hinge for the first three modes.

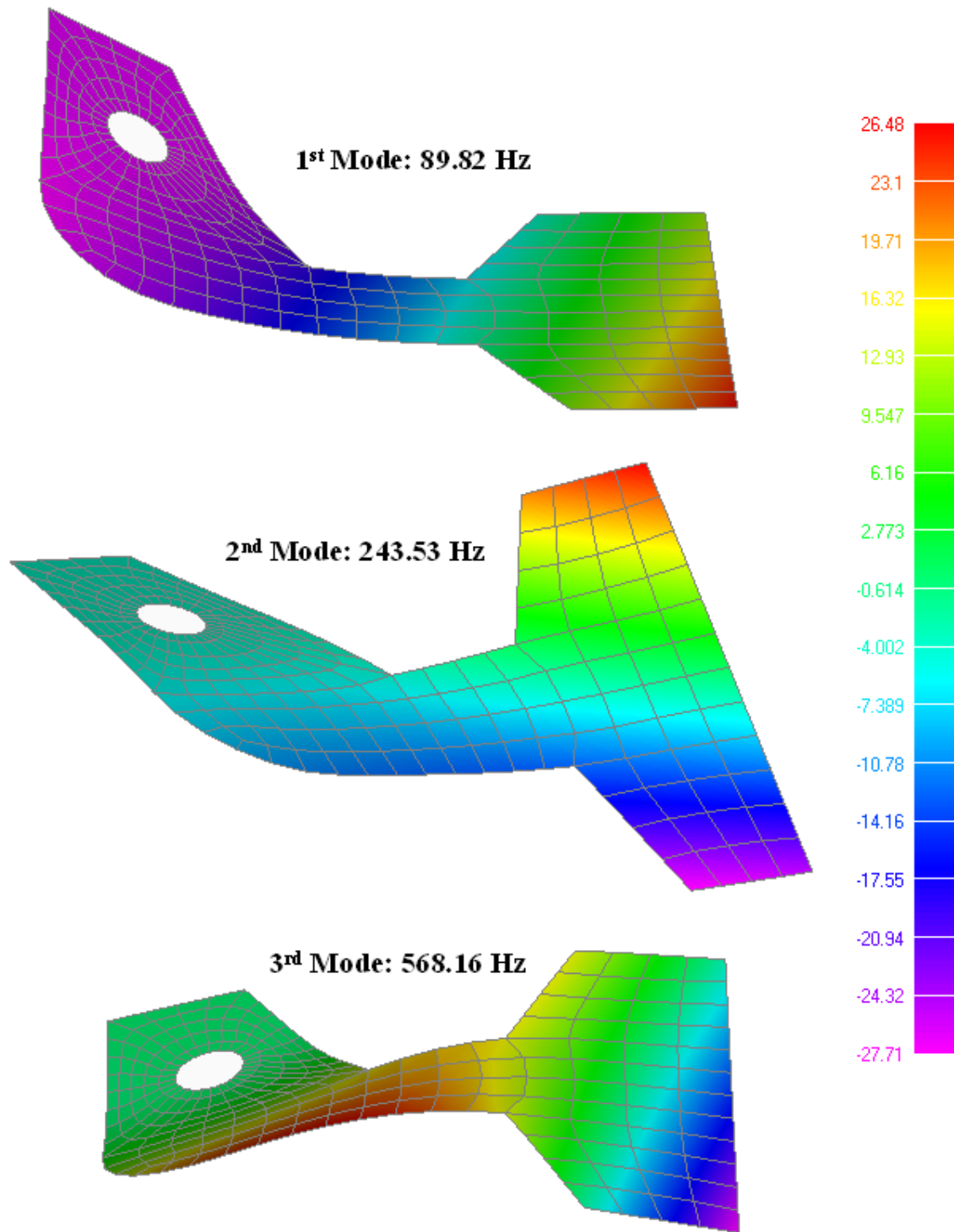


Figure 4.2. Deformed and contoured representations of the mode shapes for the first three modes of vibration of the hinge plate.

As with the simple one degree-of-freedom spring mass system, it is necessary to first perform a time-domain analysis as a basis of comparison. Based on the lessons learned from the spring mass system, about 16 points per wavelength are needed to accurately represent a waveform for the highest mode of interest. To accurately represent 568.16 Hz, the time spacing must be at least $\Delta t = 0.00011$ second. To reduce any effects of a start-up transient due to the forcing function, Δt in Femap is selected to be 0.000025 second. However, the output interval for the data will only be 4. That is, only every fourth data point will be output. Therefore, the real Δt is 0.0001 second, which still falls within the $\Delta t < 0.00011$ second limitation imposed by the highest mode of interest. The resulting impulse forcing function for the structure is shown graphically in Figure 4.3.

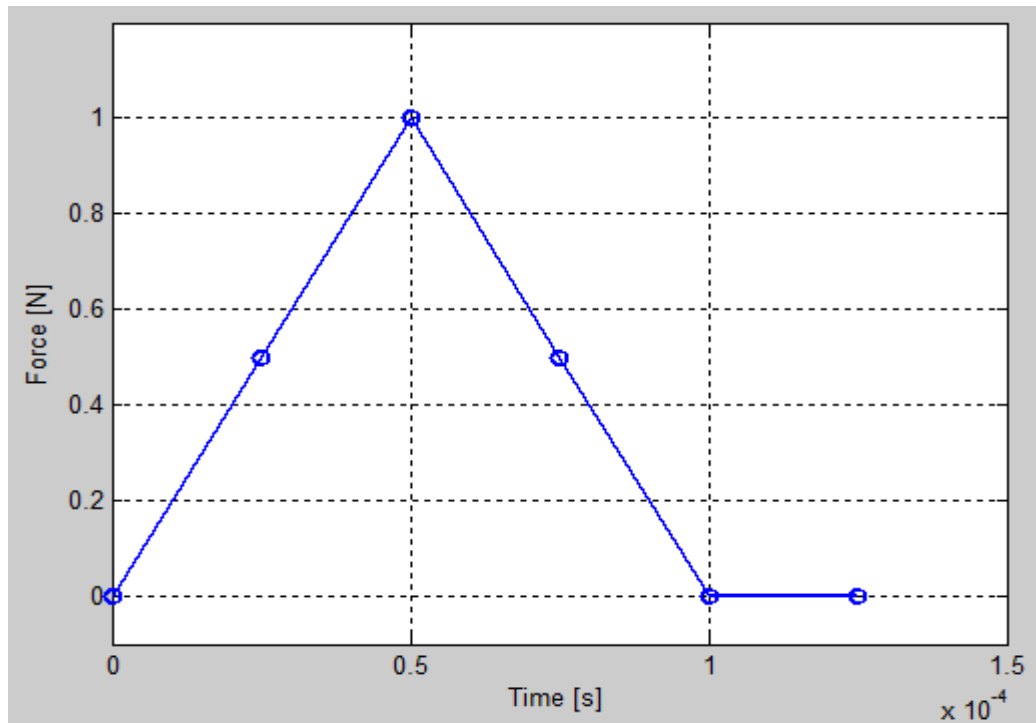


Figure 4.3. Representation of the time-domain forcing function for the hinge plate.

This forcing function will be applied at node 44 on the hinge plate model in the positive translational z-direction, which is normal to the plate surface. Node 44 is located at the bottom right corner of the hinge plate, as illustrated in Figure 4.4.

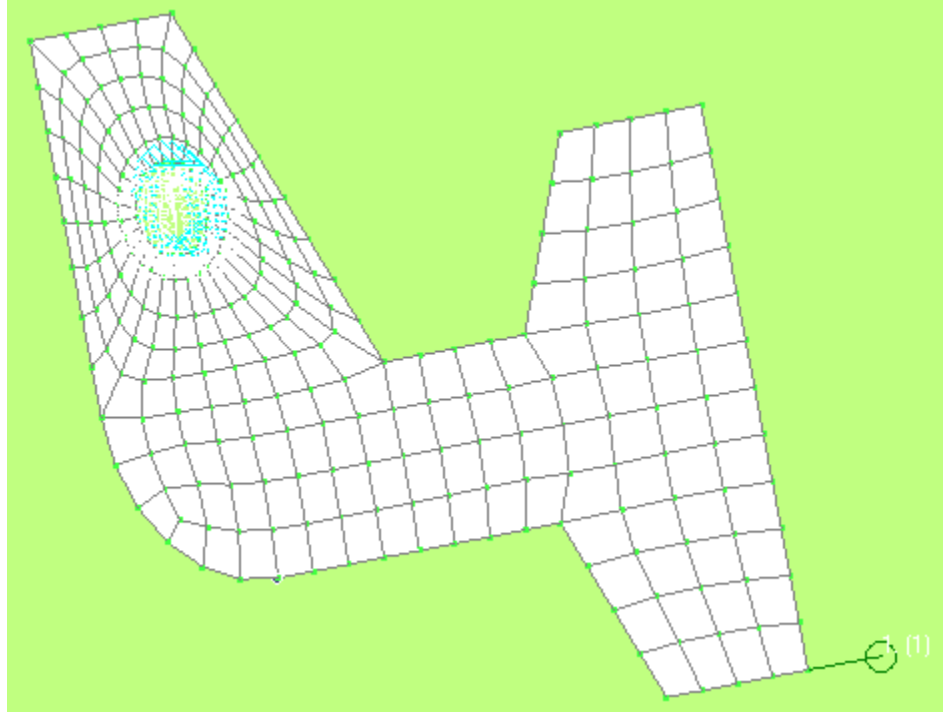


Figure 4.4. Hinge plate model shown with constraints around the hole and forcing function at node 44.

The final two parameters to set are the damping and the total length of the time record. The damping is assumed to be viscous, and is set to $\eta = 0.05$ at 600 Hz. The total length of the sample is important because the total length in the time-domain is equivalent to the frequency resolution Δf in the frequency-domain. A longer time sample equates to a finer frequency resolution. Having a longer time sample is useful since comparisons need to be made between the time-domain data and the frequency-domain data in the frequency-domain. This longer time sample will provide a more accurate answer when the data is transformed to the frequency-domain. The time analysis is taken to be 5 seconds long, which yields a frequency resolution of 0.2 Hz in the frequency-domain.

The system is now solved using NASTRAN's "direct transient" solver. The resulting time-domain output has 50,000 points with $\Delta t = 0.0001$ second, for a total duration of 5 seconds. This output is displayed in Figure 4.5.

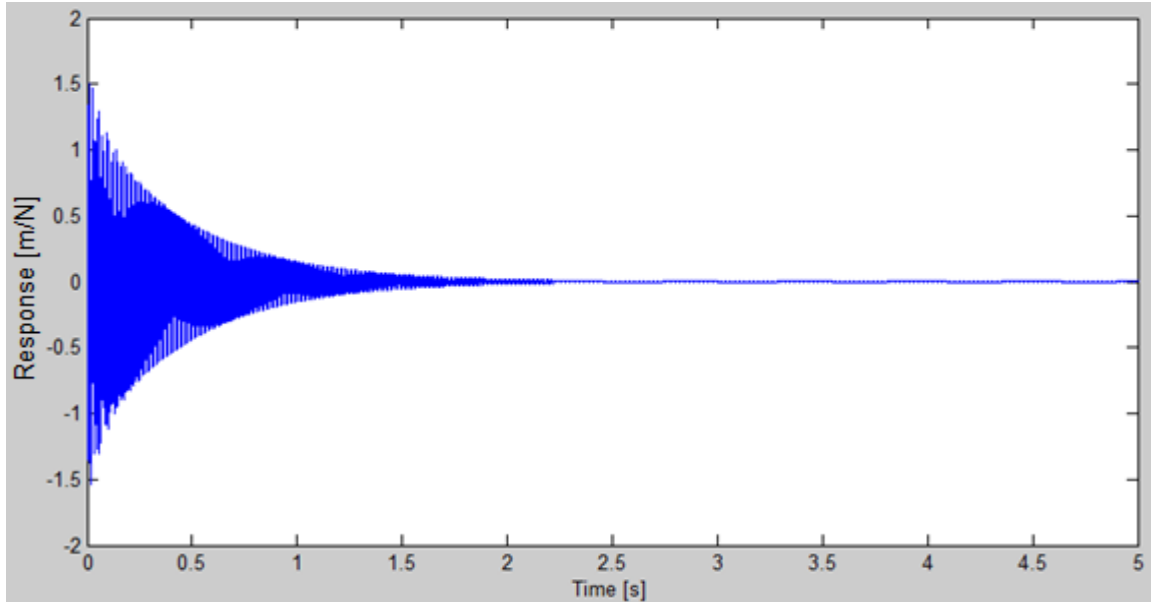


Figure 4.5. Full time-domain response of hinge plate.

When this time-domain result is transformed into the frequency-domain using the Fourier transform, the first three modes are clearly present, as well as the fact that with viscous damping, the peaks widen out as frequency increases. This is an important point to illustrate since in the frequency-domain analyses, Δf must be selected based on the sharpest peak. The resulting frequency-domain spectrum is shown in Figure 4.6.

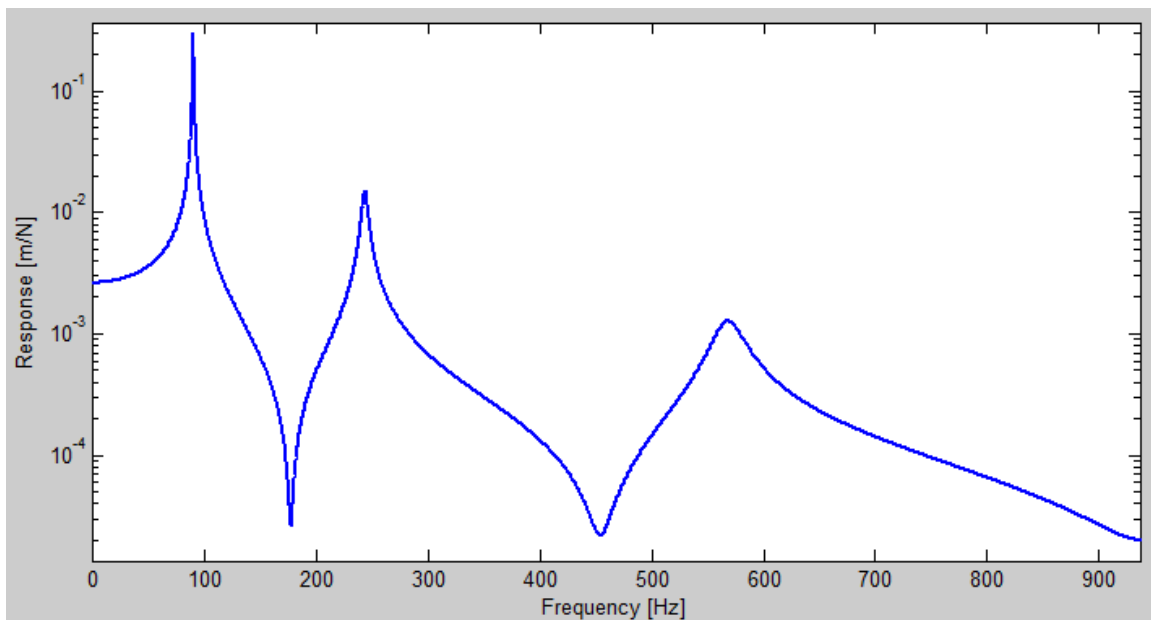


Figure 4.6. Frequency-domain representation of hinge plate time-domain results.

Zooming in on Figure 4.4, the next three plots display portions of the time-domain data associated with the first three modes of the hinge. The response in Figure 4.7 is dominated by the 89.82 Hz frequency which makes up the bulk of the time-domain plot. Over the range shown in Figure 4.8, the second mode at 243.53 Hz dominates the response. Figure 4.9 is the most important and shows the data heavily influenced by the third 568.16 Hz mode. Even at this high frequency, the 568.16 Hz waveform is still represented by about 16 points per wavelength, and can serve as a clean comparison for the transformed frequency-domain results.

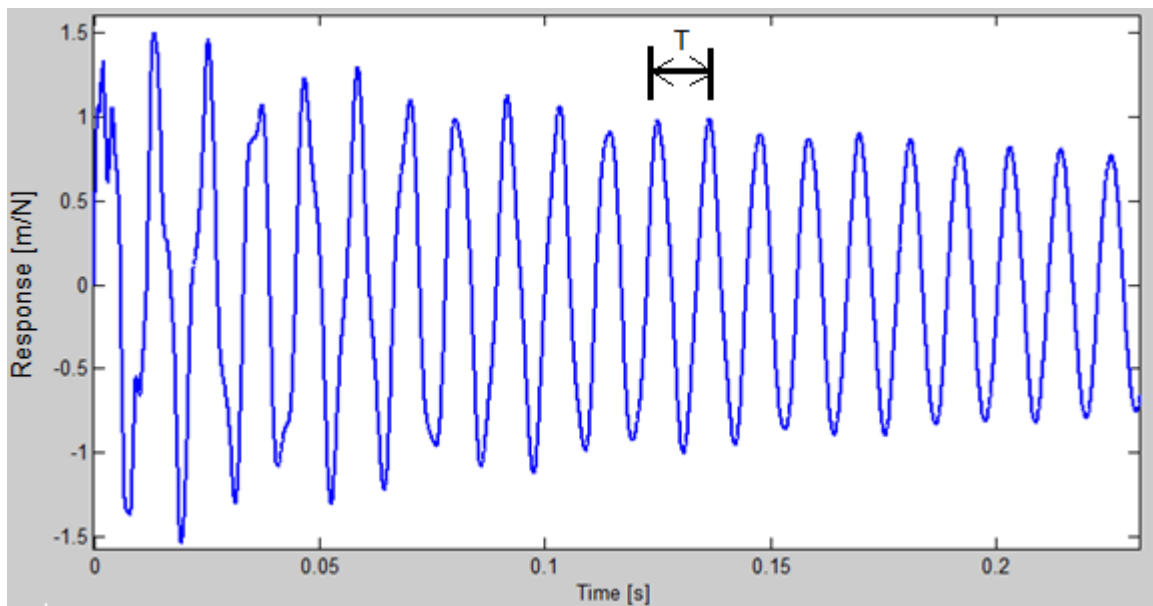


Figure 4.7. Time-domain representation of hinge plate solution highlighting the first mode, where the period $T = 0.0111$ second, whose reciprocal equals 89.82 Hz.

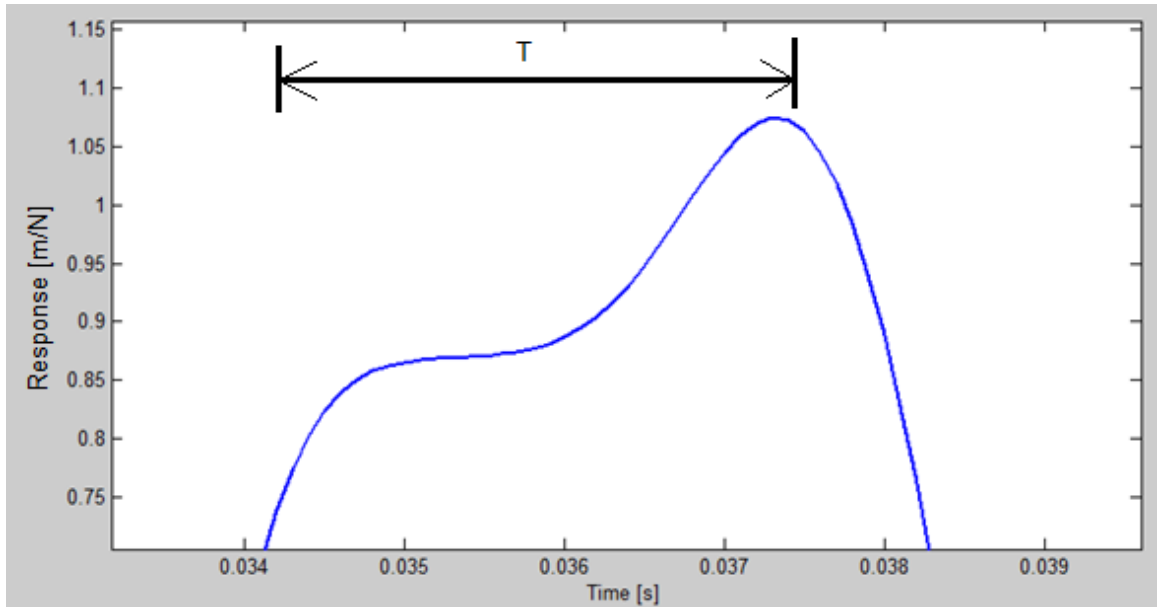


Figure 4.8. Time-domain representation of hinge plate solution highlighting the second mode, where the period $T = 0.004$ second, whose reciprocal equals 243.53 Hz.

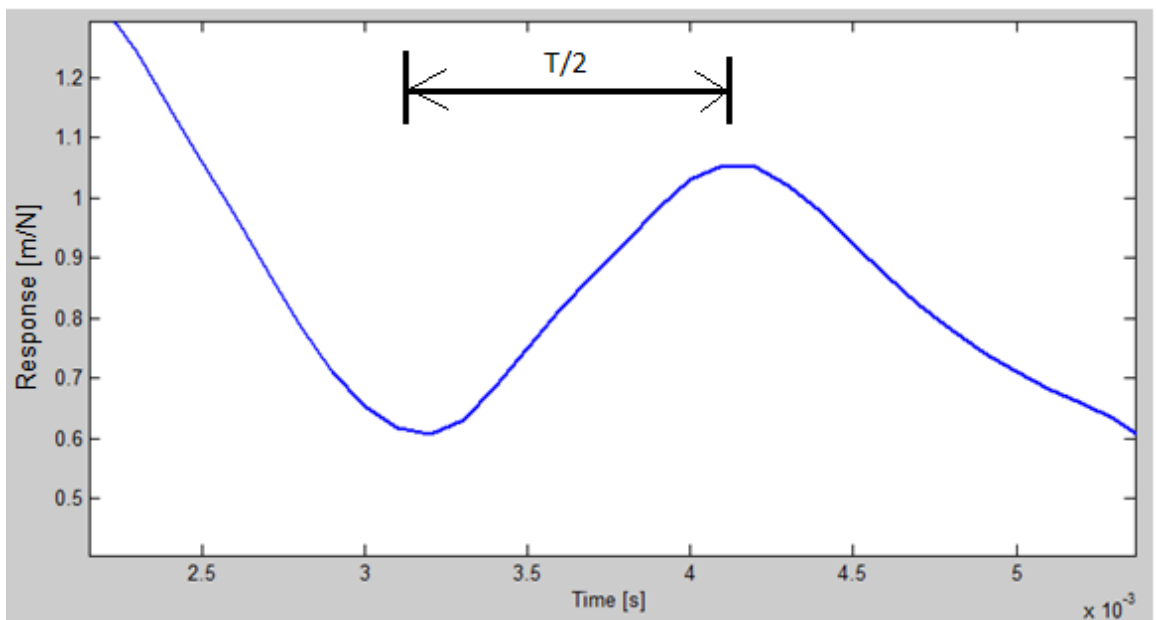


Figure 4.9. Time-domain representation of hinge plate solution highlighting the third mode, where the period $T = 0.00176$ second, whose reciprocal equals 568.16 Hz.

Similar to the simple spring mass system, comparisons will be made between the time-domain data found above, and transformed frequency-domain data computed using NASTRAN's "modal frequency" solver. To make a direct comparison, the forcing function and damping conditions are taken to be the same for the frequency-domain

analyses as they were for the time-domain analysis. For the time-domain analysis, the viscous damping condition was set to $\eta = 0.05$ at 600 Hz. For the frequency-domain analyses, a damping function must be created that is equivalent to the time-domain damping. Table 4.2 contains the values selected to represent viscous damping in the system.

Table 4.2. Values representing the viscous damping function for the frequency-domain analyses of the hinge plate.

Frequency [Hz]	Loss Factor η
0	0
600	0.05
2000	0.16666

Since we are only interested in the first three modes of the hinge plate, it is necessary to extend the damping function up to a much higher frequency than the final mode of interest. This ensures that the higher modes we aren't interested in will be sufficiently damped by the viscous damping condition. Figure 4.10 is a graphical representation of the viscous damping function.

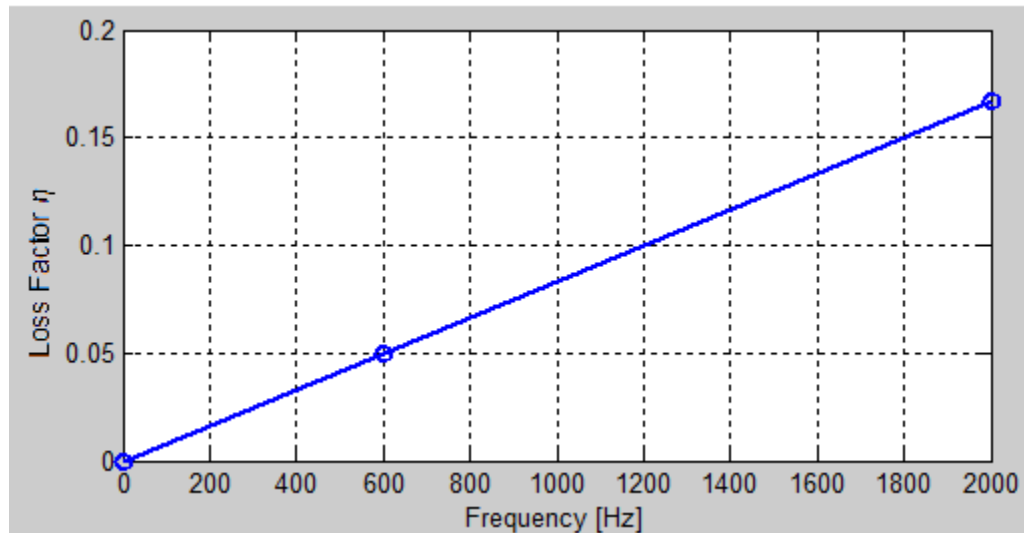


Figure 4.10. Graphical representation of the viscous damping function for the frequency-domain analysis of the hinge plate.

The forcing function for the hinge plate is very similar to the forcing function for the simple spring mass system. To capture the three modal frequencies of interest, the system is forced with a flat frequency response force of 1 N from 0 Hz to 600 Hz, as

shown in Figure 4.11. As with the time-domain analysis, the system is forced at node 44 in the lower right hand corner of the hinge plate. Node 44 is also where the displacement of the system is sampled.

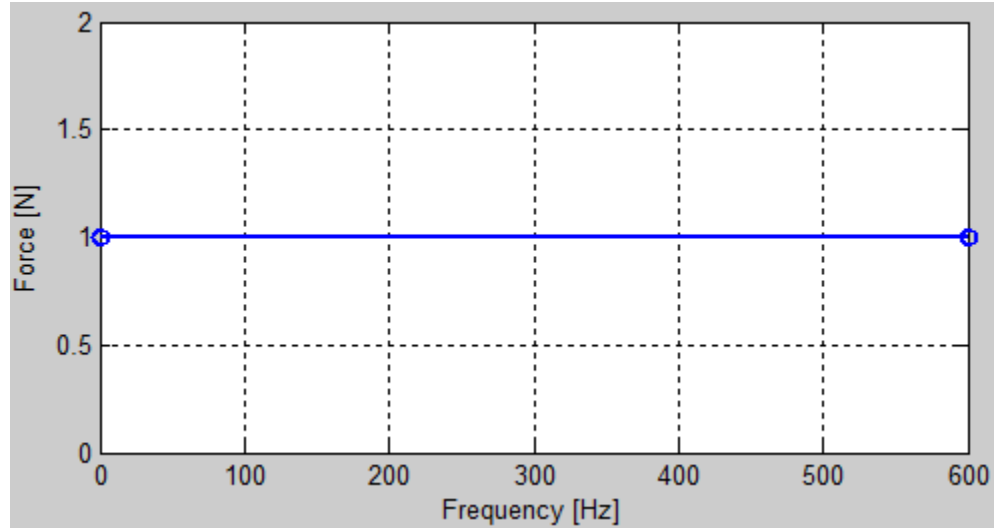


Figure 4.11. Forcing function for the frequency-domain analysis of the hinge plate.

Since the frequency range in the frequency-domain determines the sample rate Δt in the time-domain, it is important to choose the upper frequency appropriately so the highest mode of interest is accurately represented after transformation to the time-domain. The highest mode of interest is 568.16 Hz. Since we determined earlier that 16 points per wavelength is an appropriate number of points to accurately represent a waveform, multiplying 568.16 Hz by 16 will result in the frequency range for the frequency-domain analyses. This multiplication gives a result of about 9000, so the frequency range of all further frequency-domain analyses will be 9000 Hz, which sets the actual upper frequency for the NASTRAN analysis to 4500 Hz. The complex conjugate of the NASTRAN output is then reflected across the y-axis to produce the full linear spectrum as described in Chapter 2.

As displayed previously in Figure 4.6, the mode with the sharpest peak is the first mode at 89.82 Hz. Since Δf for frequency-domain analyses should be set by the sharpest peak, its value must be calculated at this point. For the first mode, $f = 89.82$ Hz, and since $\eta = 0.05$ at 600 Hz, $\eta = 0.0075$ at 89.82 Hz. So given the equation $\Delta f < \eta * f$, multiplying η and f results in a value of $\Delta f = 0.67$ Hz. Based on the results of the spring

mass system from Chapter 3, it is expected that the amplitude of the transformed frequency-domain data will begin to decrease near the point where $\Delta f = 0.5(0.67)$ Hz for a frequency-domain analysis.

Given this information, three frequency-domain analyses are performed that show the breakdown in the overall amplitude of the time-domain waveforms for an increasing Δf . The parameters for the first analysis are $\Delta f = 0.2$ Hz with a frequency range of 9000 Hz. Figure 4.12 shows a portion of this first analysis, transformed into the time-domain using the *ifft* command in Matlab, compared to the original “direct transient” time-domain results.

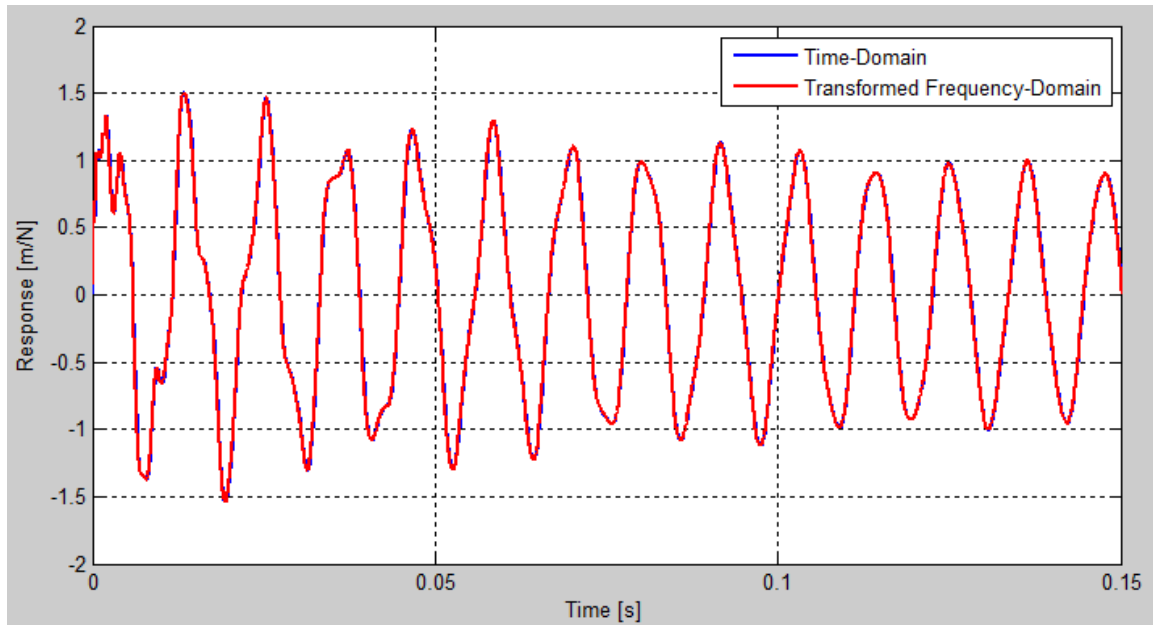


Figure 4.12. Transformed frequency-domain representation with $\Delta f = 0.2$ Hz and frequency range = 9000 Hz, compared to Femap time-domain representation.

Figure 4.12 shows the two curves to be nearly identical. The parameters for the second analysis are $\Delta f = 0.6666$ Hz with a frequency range of 9000 Hz. This Δf value is very close to the Δf value of 0.67 Hz specified by the $\Delta f < \eta * f$ equation.

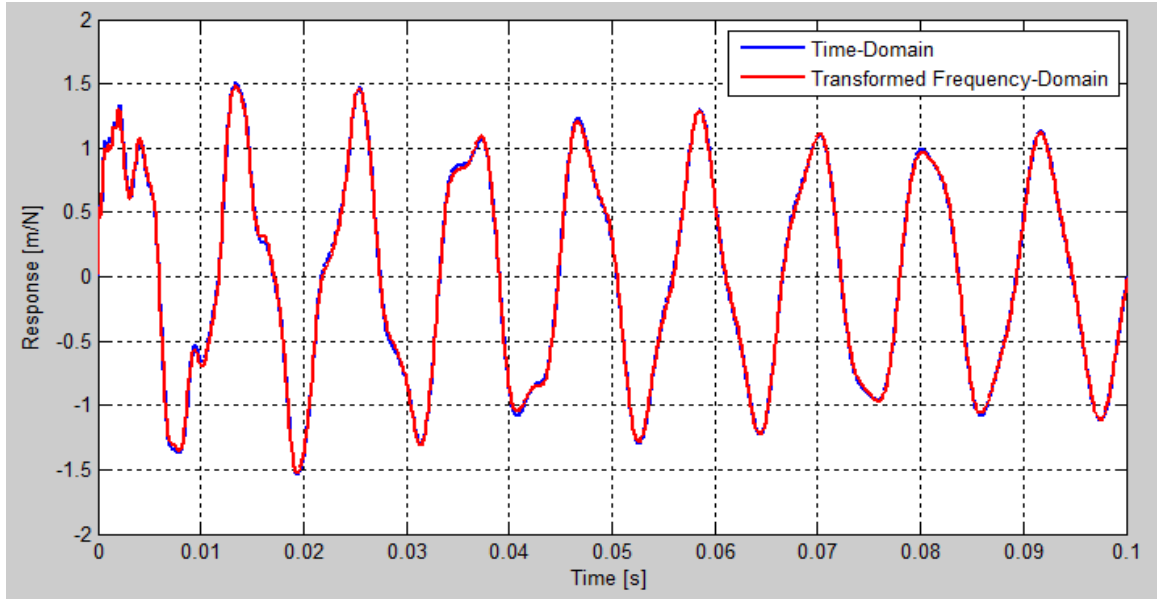


Figure 4.13. Transformed frequency-domain representation with $\Delta f = 0.6666$ Hz and frequency range = 9000 Hz, compared to Femap time-domain representation.

The upper limit for the time has been reduced in Figure 4.13 to highlight the fact that the amplitude of the transformed frequency-domain curve starts to decrease in relation to the time-domain curve. The parameters for the third analysis, shown in figure 4.13, are $\Delta f = 1.3333$ Hz with a frequency range of 9000 Hz. Since this Δf value is well above $\Delta f = 0.67$, a severe degradation of the amplitude is clearly visible.

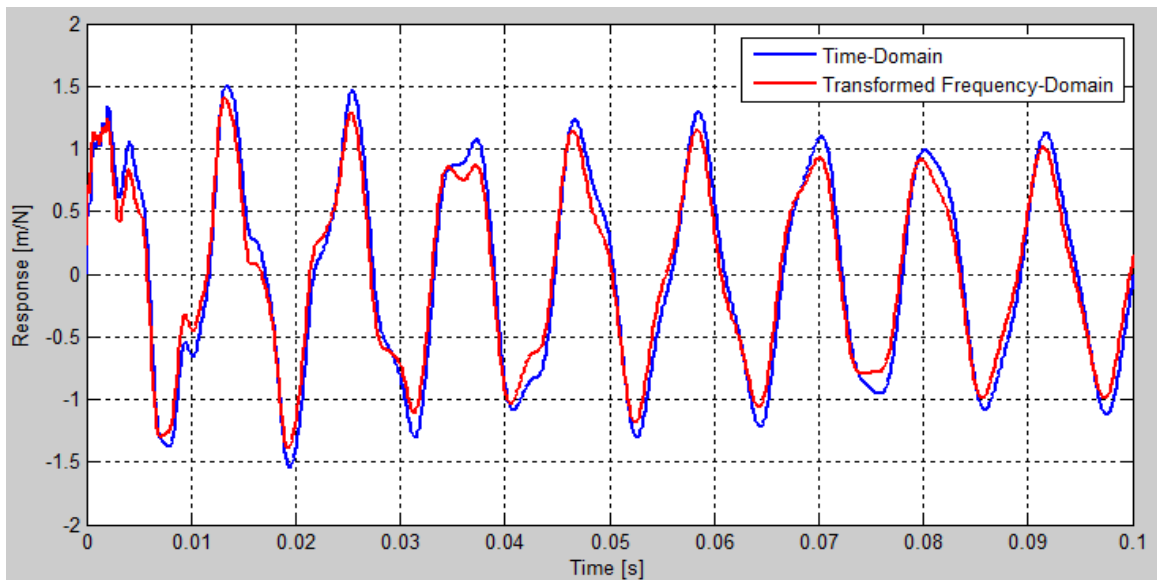


Figure 4.14. Transformed frequency-domain representation with $\Delta f = 1.3333$ Hz and frequency range = 9000 Hz, compared to Femap time-domain representation.

For Figures 4.12, 4.13 and 4.14, the response is dominated by the first mode at 89.82 Hz. But even as Δf is increased from 0.2 Hz to 1.3333 Hz, the amplitudes of the higher mode components of the waveform are not affected. This fact is certainly not obvious in the time-domain, so it will be demonstrated in the frequency-domain by transforming NASTRAN's "direct transient" time output into the frequency-domain using Matlab's *fft* command. Figure 4.15 compares the transformed time-domain solution, and the $\Delta f = 0.6666$ Hz frequency-domain solution for the first three modes of the hinge plate. As expected, the two curves resemble each other very closely.

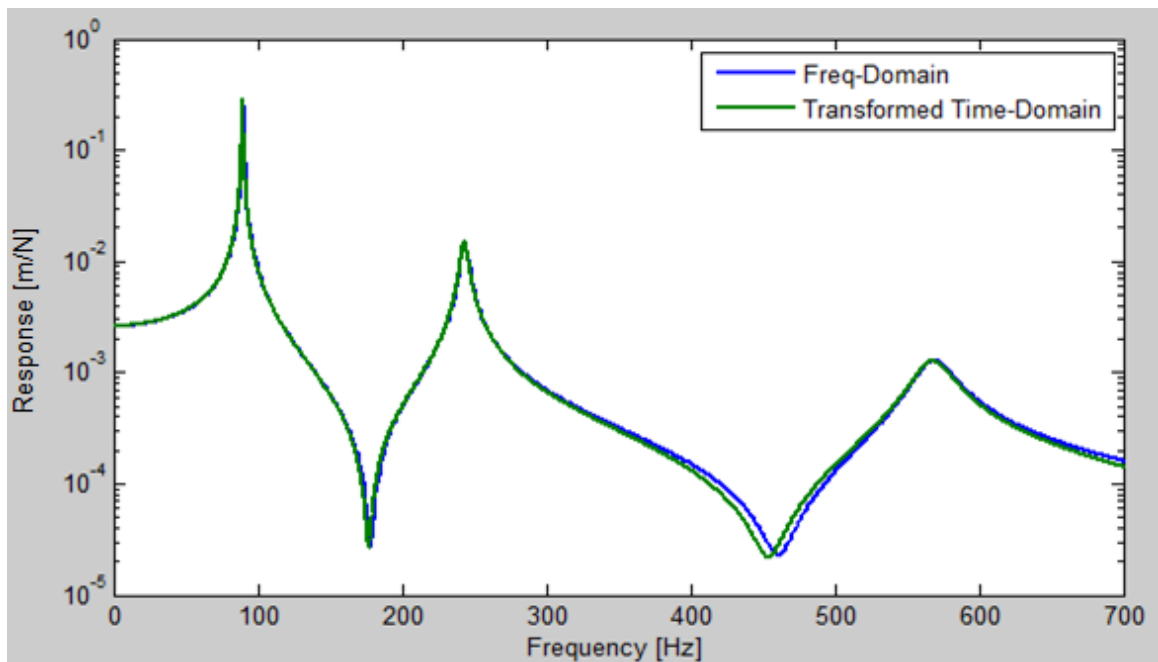


Figure 4.15. Frequency-domain comparison between frequency-domain data at $\Delta f = 0.6666$ Hz and transformed time-domain data.

Figure 4.16 contains the same two curves as Figure 4.15, but is zoomed in on the first mode to show the differences in resolution near the first resonance peak for the two curves.

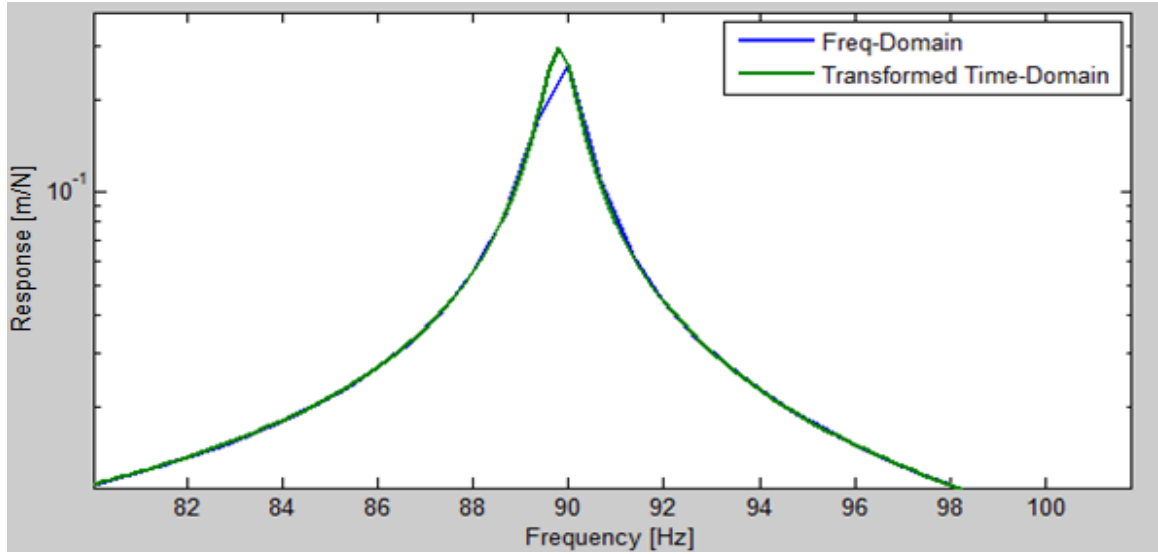


Figure 4.16. Frequency-domain comparison between frequency-domain data at $\Delta f = 0.6666$ Hz and transformed time-domain data focused on the first mode.

Similarly, Figure 4.17 shows the two curves for the third resonance peak. The slight difference in the curves is likely due to mode truncation for the modal frequency response calculations since the transformed time-domain data was calculated using a “direct transient” response analysis that includes all the modes and represents the correct solution. However, this slight variation does not affect the comparisons between the amplitudes of the two curves.

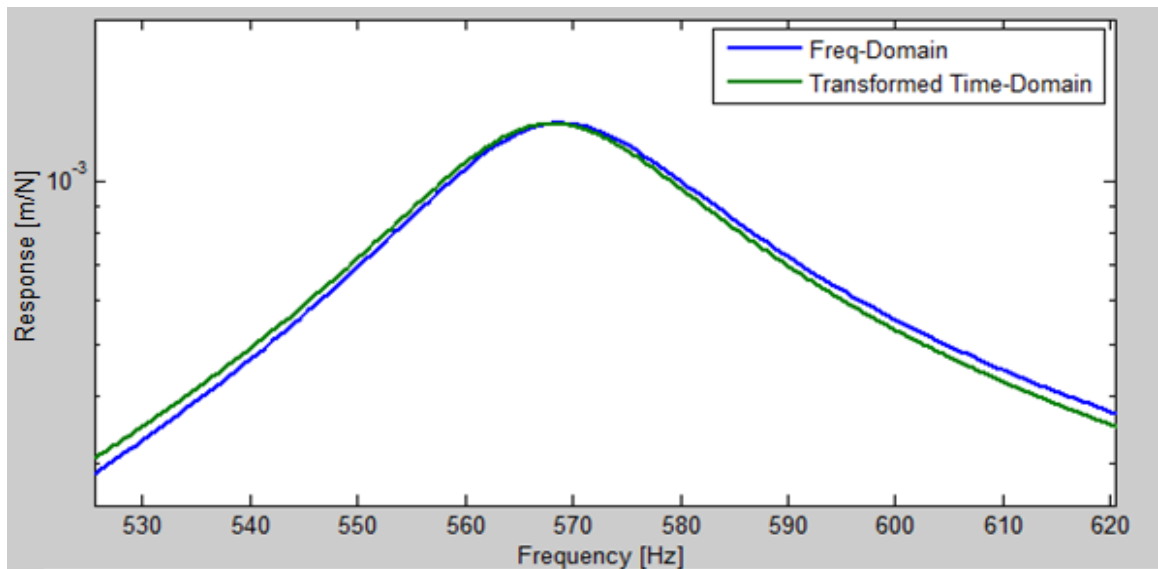


Figure 4.17. Frequency-domain comparison between frequency-domain data at $\Delta f = 0.6666$ Hz and transformed time-domain data focused on the third mode.

Figure 4.18 shows a comparison between the transformed time-domain solution and the frequency-domain solution with $\Delta f = 1.3333$ Hz near the first mode of the hinge plate. Since the frequency spacing is larger than the $\eta * f$ value at this peak, the amplitude difference between the transformed time-domain solution and the frequency-domain solution is greater than that shown in Figure 4.16, where the Δf value for the frequency-domain solution was very close to the $\eta * f$ value.

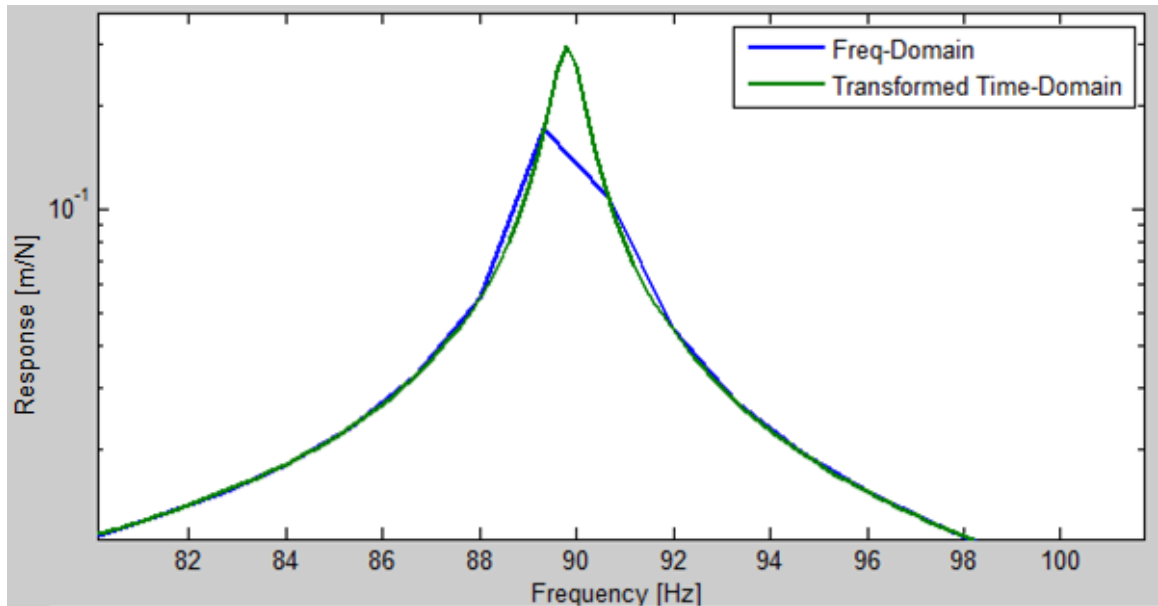


Figure 4.18. Frequency-domain comparison between frequency-domain data at $\Delta f = 1.33333$ Hz and transformed time-domain data focused on the first mode.

Figure 4.19 shows the same two curves as Figure 4.18, but is zoomed in on the third mode.

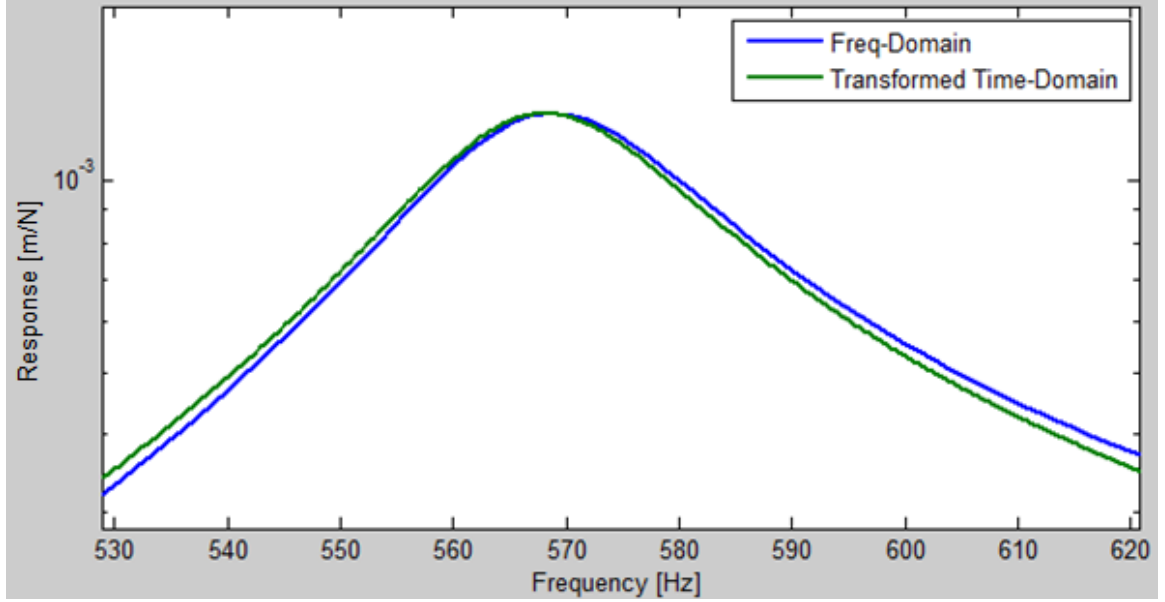


Figure 4.19. Frequency-domain comparison between frequency-domain data at $\Delta f = 1.3333$ Hz and transformed time-domain data focused on the third mode.

A frequency spacing of $\Delta f = 1.3333$ Hz is clearly adequate to resolve the third peak, as is expected because $\eta^*f = 29.9$ for this mode. Although not shown, the same is true for the second mode, where $\eta^*f = 4.94$. Values of 4.94 and 29.9 are obviously much higher than 0.67, which is the calculated η^*f value for the first mode. So in order to accurately represent the components of the second and third modes in the time-domain waveform, Δf must be less than 4.94 Hz for the second mode and Δf must be less than 26.9 Hz for the third mode. Therefore, it is clear why the second and third modes would still be accurately represented when the frequency domain analysis has a Δf of 1.3333 Hz.

The above process demonstrates why it is very important to concentrate on the sharpest peak, which is the mode with the lowest η^*f value. As long as the $\Delta f < \eta^*f$ condition is met for that peak, the other modes will be accurately represented in the time-domain waveform.

Chapter 5. OTHER CONSIDERATIONS

Possible Effects of a Larger Frequency Resolution

When dealing with the modes associated with a system such as the hinge plate as described in Chapter 4, a convenient way to further reduce computation times seems to present itself. The system's first mode of vibration occurs at 89.82 Hz, and choosing $\Delta f = 1.3333$ Hz in the frequency-domain produces an insufficient time-domain response as illustrated in Figure 4.13. The shortcomings of this Δf value are also apparent in the frequency-domain as illustrated in Figure 4.17. The frequency response is sampled at 89.3333 Hz and 90.6666 Hz, which essentially cuts off the peak of the response at 89.82 Hz.

Given this unfortunate frequency spacing, it may be tempting to simply increase Δf to 1.5 Hz, which would place a sample point exactly at 90 Hz, which is very close to 89.92 Hz. Perhaps having a point very close to the modal peak will produce a better answer than the previous analysis despite the larger Δf . Figure 5.1 displays a frequency-domain comparison at the first mode between the transformed time-domain result and a frequency-domain response where $\Delta f = 1.5$ Hz. This figure contrasts with Figure 4.17 in that the peak of the mode is more closely resolved.

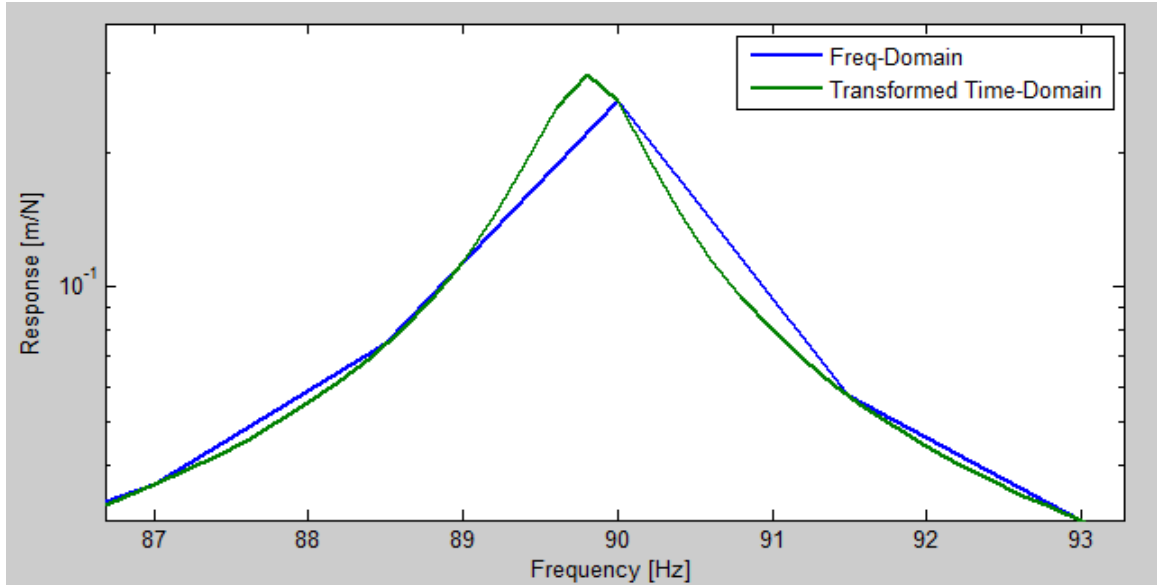


Figure 5.1. Frequency-domain comparison between frequency-domain data at $\Delta f = 1.5$ Hz and transformed time-domain data focused on the first mode.

Since the peak of the frequency-domain data is now closer to the peak of the transformed time-domain data, it might be assumed that this will produce a better correlation between the two response curves in the time-domain as opposed to the response at $\Delta f = 1.3333$ Hz. However, this is unfortunately not true. The time-domain comparison is illustrated in Figure 5.2.

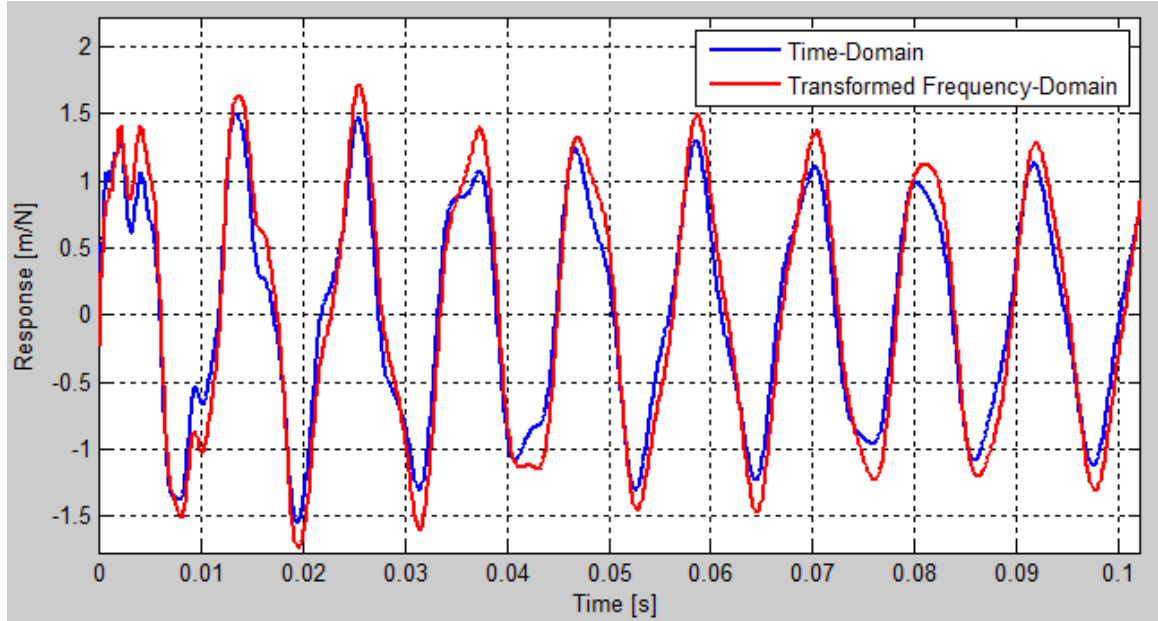


Figure 5.2. Transformed frequency-domain representation with $\Delta f = 1.5$ Hz and frequency range = 9000 Hz, compared to a time-domain in Femap.

The results in Figure 5.2 show that changing the frequency resolution for the frequency-domain solution to a value of $\Delta f = 1.5$ Hz increases its amplitude in the time-domain beyond that of the correct time-domain solution. This appreciable increase is due to how broad the peak ends up being in the frequency domain when Δf is larger. This can be seen in Figure 5.1, where the frequency-domain response is actually greater than the transformed time-domain response from about 87 Hz – 88.5 Hz, and from 90 Hz – 93 Hz.

The results in Figures 5.1 and 5.2 show that picking a larger Δf value to save computation time and assuming it will produce a good answer simply because one of the frequency points lands squarely on a peak is typically not a good practice. However, where a mode falls in relation to the frequency sample point has an impact on solution accuracy and being aware of this can assist in achieving a more accurate solution. Since the mode that contains the lowest η^*f value is known from doing NASTRAN's "normal mode/eigenvalue" analysis prior to the frequency response analysis, certain simple observations make it much easier to select an appropriate value for Δf .

In the analysis of the simple spring mass system, when the Δf value is very close to the η^*f value in Figure 3.5, the amplitude is close to, but clearly less than the time-domain amplitude. In contrast, for the hinge plate analysis, when the Δf value is very

close to the η^*f value in Figure 4.12, the amplitude is almost exactly the same as the time-domain amplitude. The explanation is that the spring mass system analysis involves the worst case scenario, where the peak in the response falls directly in between two frequency sample points, while the peak in the response for the first mode of the hinge plate is very close to a frequency sample point. In regards to the $\Delta f < \eta^*f$ rule established earlier, if the peak is directly between two frequency sample points, picking $\Delta f < \eta^*f$ should produce a reasonably accurate transformed frequency-domain solution, with the amplitude decreasing in relation to the time-domain solution the closer Δf approaches η^*f . If the peak happens to fall very close to one of the frequency points, picking $\Delta f = \eta^*f$ should produce a very good solution. In this same situation where the peak falls very close to one of the frequency points, if Δf is slightly greater than η^*f , the amplitude of the transformed frequency-domain solution will increase in relation to the time-domain solution. And if Δf isn't increased too far above η^*f , the difference in amplitude between the two curves won't be any greater than the difference in amplitude between the two curves when Δf is slightly less than η^*f for the scenario where the peak is directly between frequency sample points. This point is illustrated by the fact that in Figure 4.12, Δf is nearly identical to η^*f , and the amplitudes are essentially the same. But in Figure 3.8, Δf is less than η^*f , but the amplitude of the transformed frequency-domain response is visibly slightly less than the time-domain response.

So essentially, it is possible to get away with Δf being slightly greater than η^*f , but only if the modal peak is very close to a frequency sample point. Knowing this can give us additional insight when choosing a Δf value. For example, if the mode of a system exists at $f = 99$ Hz, where $\eta = 0.05$ at that frequency, this makes $\eta^*f = 4.95$ Hz. Choosing $\Delta f = 4.83$ Hz which is less than 4.95 Hz to adhere to the $\Delta f < \eta^*f$ rule, frequency samples points occur at 96.6 Hz and 101.43 Hz. This selection places 99 Hz almost directly in between the two frequency sample points, and there will most likely be a visually apparent difference between the transformed frequency-domain curve and the time-domain curve, with the transformed frequency-domain curve having slightly lower amplitude. However, if Δf is increased to 5 Hz, which is only slightly higher than the η^*f value of 4.95 Hz, the transformed frequency-domain curve will still be very accurate in relation to the time-domain curve, but its amplitude will be slightly higher than the time-

domain curve. So, both solutions will be relatively accurate, but the solution using $\Delta f = 5$ Hz is less computationally expensive. But again, as stated earlier, the required solution accuracy will also depend on the particular application, and depending on whether the analysis is used for design iterations or final numerical computations.

Further Reduction of Computation Times

As noted previously, the frequency range for the frequency-domain solution determines the time resolution in the time-domain. Allowing the analysis to be completed up to a specified frequency range ensures that the highest mode of interest will be accurately represented once the result is transformed to the time-domain. For the hinge plate analysis, the third mode at 568.16 Hz is the highest mode of interest, and requires a frequency range of 9000 Hz to fully represent the shape of the waveform with about 16 points per wavelength in the time-domain. Of course, the analysis in Femap only includes frequencies up to 4500 Hz. The rest of the linear spectrum was obtained by mirroring this data and taking the complex conjugate to fill it out to 9000 Hz. Once the full linear spectrum is established, the Matlab *ifft* command can be performed to obtain a time-domain result.

Fortunately, it is not necessary to actually perform the analysis all the way up to 4500 Hz in Femap. Taking advantage of this can save a significant amount of computation time. While precise documentation of the savings in computation time would be advantageous, this example problem is so small in relation to real-world problems that it doesn't make sense to establish time savings based on such a small model. Figure 5.3 displays the full linear spectrum for the Femap output of the frequency-domain analysis with $\Delta f = 0.6666$ Hz.

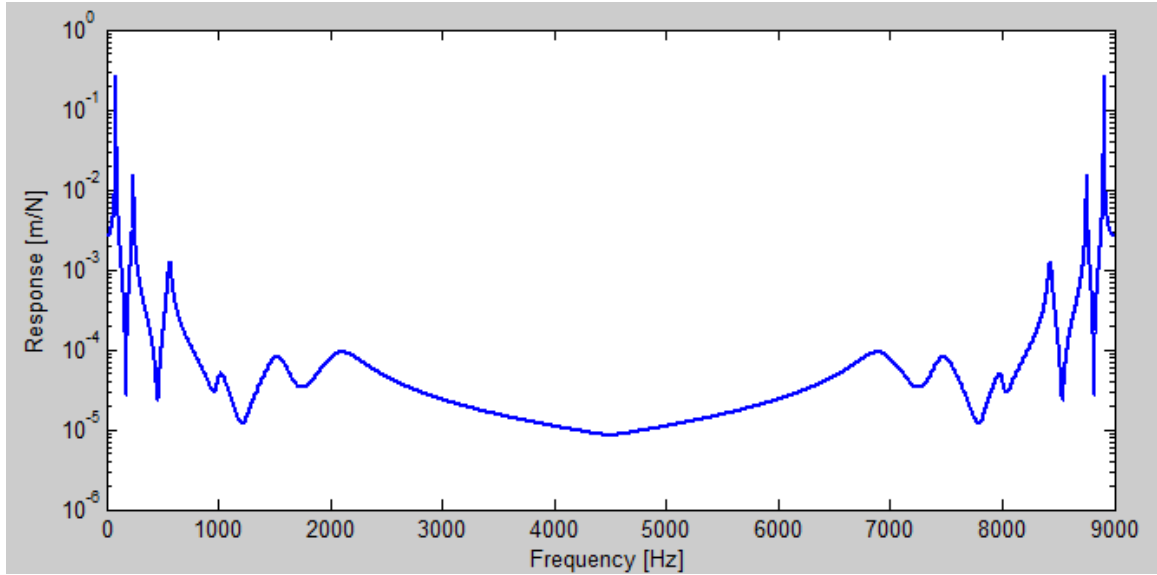


Figure 5.3. Linear spectrum for the Femap output of the frequency-domain analysis with $\Delta f = 0.6666$ Hz.

Since the frequency range of interest only includes the first three modes, based on Figure 5.3, it should follow that any response between about 1000 Hz and 8000 Hz is negligible and should have no bearing on the final time-domain representation of this data. To show that this is true, the linear spectrum will be reconstructed using only the data collected from 0 Hz to 1200 Hz. The new spectrum will include the original data from 0 Hz to 900 Hz. Then, to ensure a smooth transition, the original data from 900 Hz to 1200 Hz is multiplied by the shape of the second half of a Hanning window. That is, the data point at 900 Hz is multiplied by 1, and the data point at 1200 Hz is multiplied by 0, with the points in between essentially following the smooth and gradual decline of the second half of the Hanning window. Between 1200 Hz and 7800 Hz, the spectrum is filled in with zeros for all data points. The final section between 7800 Hz and 9000 Hz is the mirrored complex conjugate of the section between 0 Hz and 1200 Hz of the new reconstructed linear spectrum. Figure 5.4 illustrates the new reconstructed spectrum.

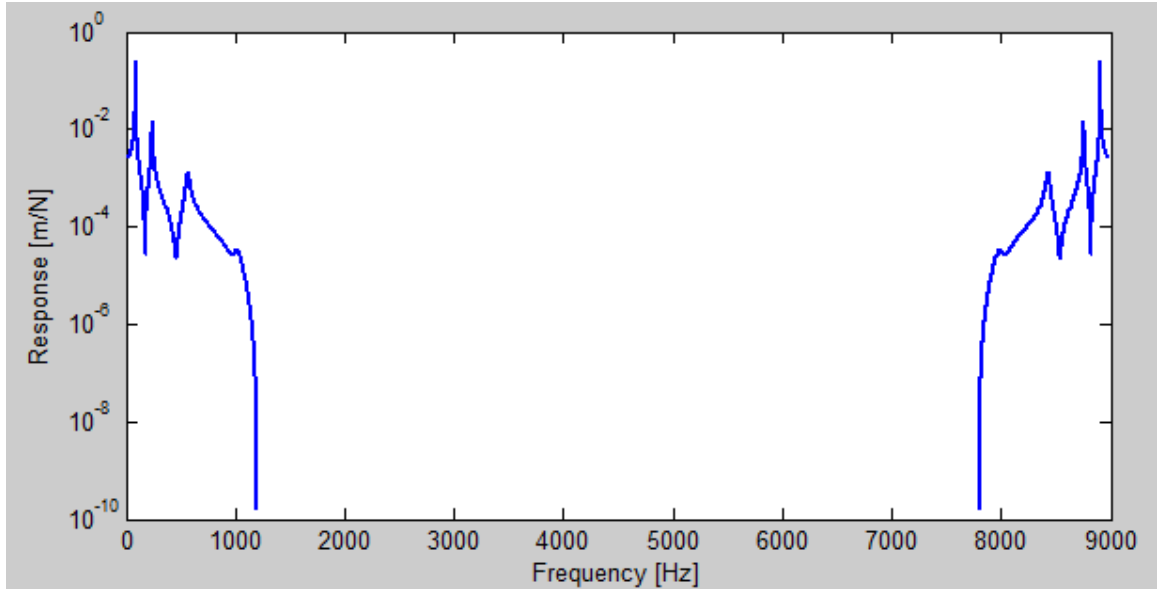


Figure 5.4. Linear Spectrum of frequency-domain data with $\Delta f = 0.6666$ Hz, with Femap frequency sampled up to 1200 Hz.

When the linear spectra in Figures 5.3 and 5.4 are transformed into the time-domain, they produce the same result, which is illustrated in Figure 5.5.

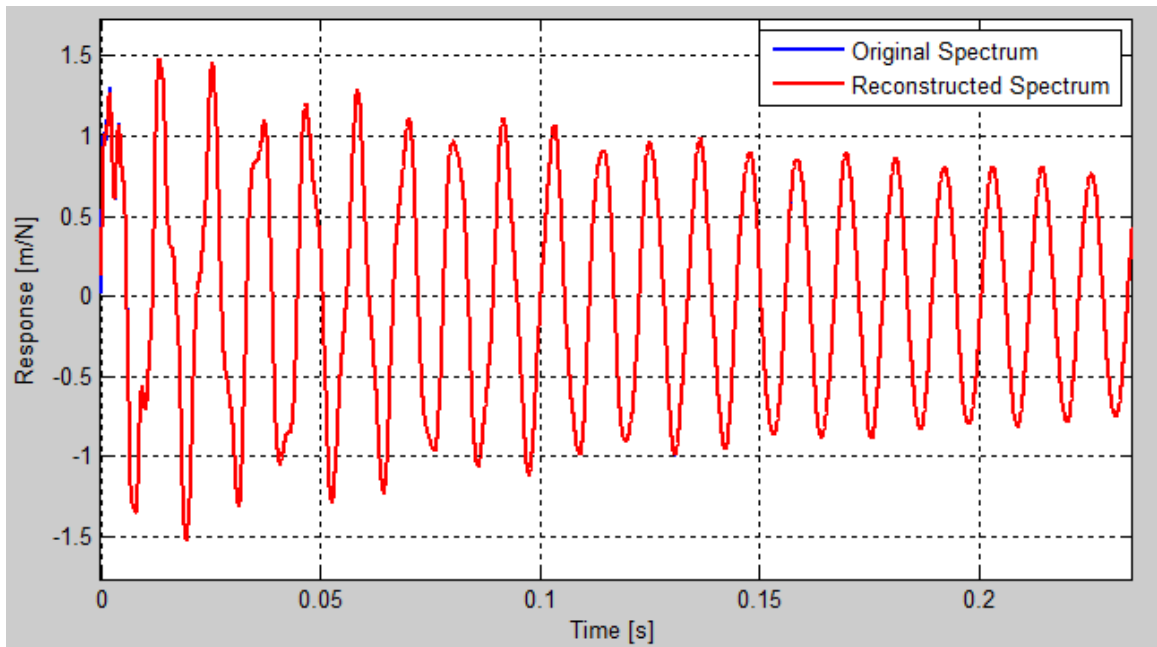


Figure 5.5. Comparison of time signals computed with the original transformed spectrum and the reconstructed transformed spectrum.

The small discrepancy between the curves at the very beginning of the response in Figure 5.5 occurs because higher frequencies weren't completely damped in Femap for

the original frequency-domain analysis. Otherwise, as expected, the response of the two time-domain curves is exactly the same, and is why the plot appears to show only one curve. The similarity discovered between the two curves in Figure 5.5 has a very profound impact on the amount of computation time needed to produce accurate results. For this specific example, the frequency range sampled in Femap only needs to be about one quarter of the original frequency range. The rest of the linear spectrum can be easily constructed from Femap's output using a simple Matlab routine. Therefore, once the highest mode of interest is determined, the maximum analysis frequency in Femap can be chosen to be about 1.6 times higher than the peak of this highest mode, and then the rest of the spectrum can be fabricated in Matlab up to the frequency range required to accurately display the waveform of the highest mode of interest in the time-domain.

Extended Period

When selecting frequency resolution for analyses in the frequency-domain, it is not only important to consider the error in the resulting time-domain amplitude, but to also consider the total length of the transformed results, since frequency resolution in the frequency-domain determines overall length in the time-domain. The term “extended period,” as described in Martins et al.,³ comes from the idea that the Fourier transform assumes a system is both forced and responds periodically in time. In order to transform data from the time-domain into the frequency-domain using the FFT, the total time sample must be extended until it is completely damped so that it obeys the causality condition for responses to a non-periodic loading. However, the idea of an extended period is also helpful in selecting the frequency resolution for frequency-domain analyses. The extended period T_p may be predicted using:

$$T_p \geq \frac{\ln(100/h)}{2\pi * f * \eta}, \quad \text{Eq. (5.1)}$$

where η is the loss factor, f is the dominant mode of the system, and h is a percentage of the initial displacement contribution of the dominant mode. Most often, 1% is considered an acceptable value for h , but can be set based on the goals of an individual project. Equation 5.1 allows us to predict a value for frequency resolution based on what percentage of the original displacement amplitude we want remaining at the end of the

time-domain response. To illustrate the usefulness of this equation, the simple spring mass system with a viscous damping condition will be used. The modal frequency of the system is 100 Hz, and the damping at 100 Hz equals 0.14325. The $\eta * f$ value is 14.325 Hz, which means Δf should be less than 14.325 Hz. Therefore, values of $\Delta f = 8.3333$ Hz and $\Delta f = 12.5$ Hz should each produce accurate amplitudes for the responses when transformed into the time-domain.

If we assume that $h = 0.01$, or 1 %, is an acceptable percentage, solving for T_p with $f = 100$ Hz and $\eta = 0.14325$, $T_p = 0.102$ seconds. That is, the response of the system must be calculated for 0.102 seconds after the initial force impulse for the displacement amplitude of the dominant mode to dampen to 1% of its initial contribution. Taking the reciprocal of 0.102 second yields a frequency resolution of $\Delta f = 9.8$ Hz. Therefore, the frequency resolution for the frequency-domain analyses must be less than or equal to 9.8 Hz in order to yield a time-domain response where the contribution from the dominant mode is damped to 1% of its original amplitude. So it is evident that while the values of $\Delta f = 8.3333$ Hz and $\Delta f = 12.5$ Hz can both produce accurate amplitudes, only the $\Delta f = 8.3333$ Hz frequency resolution produces a sufficient extended period, which is demonstrated in Figure 5.6.

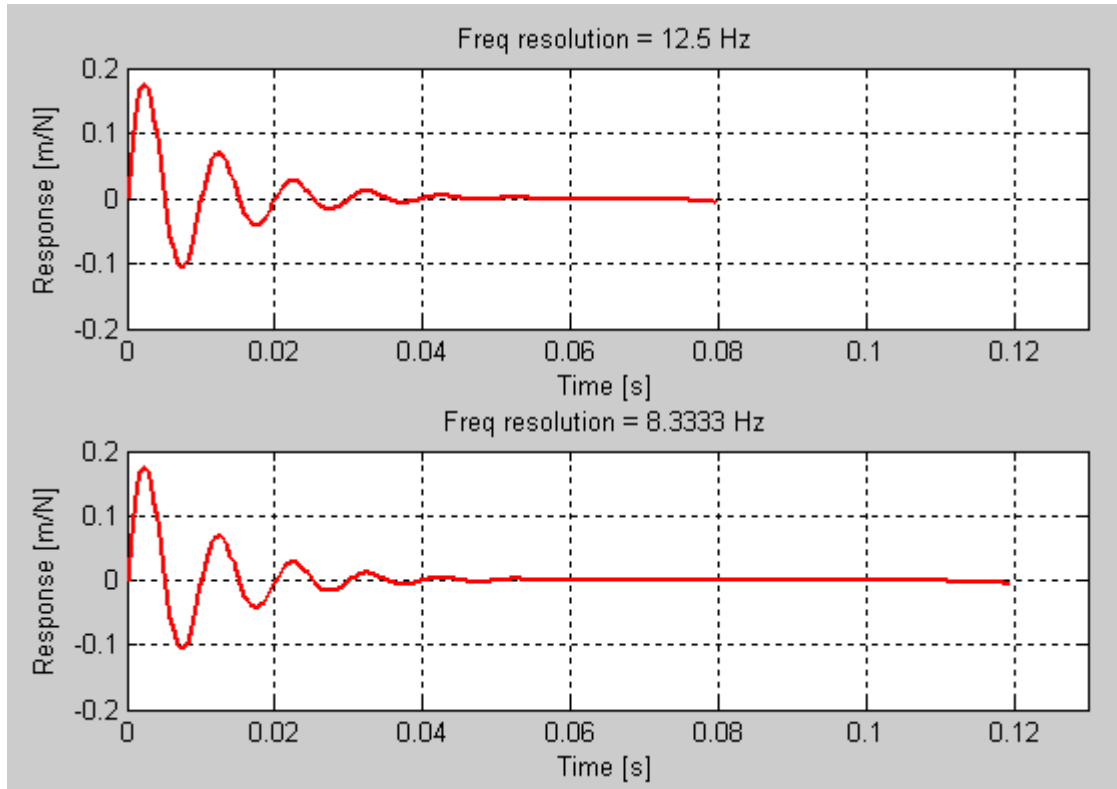


Figure 5.6. Transformed frequency-domain representation with 100 Hz modal frequency and 12.5 Hz and 8.3333 Hz frequency resolutions, where extended periods = 0.08 seconds and 0.12 seconds.

The simple example displayed in Figure 5.6 demonstrates the fundamental difference between the two frequency resolutions and how they alter the total length of the time sample. So even though the response generated with a frequency resolution of 12.5 Hz may obey the $\eta * f$ requirement, it does not meet the extended period condition of the mode damped to 1% of its original contribution at 0.102 second. Instead, the frequency resolution will have to be decreased to uphold the residual amplitude requirement.

Chapter 6. CONCLUSIONS

It is very important to be able to effectively compute the response of a structure to time-varying loads. Given the existing infrastructure which utilizes frequency-domain matrices for structural radiation problems, the purpose of this thesis was to generate general guidelines for deriving accurate time-domain responses from frequency-domain calculations. Unique factors that affect the analysis for these types of problems include the damping in the system, the modal frequencies and the frequency range of interest for the analysis.

When running a “modal frequency” analysis, the general guideline is to choose the upper frequency for the “normal modes/eigenvalue” analysis to be at least about 1.6 times the highest frequency of interest. The highest mode of interest will have the smallest period of all the modes once the response is transformed to the time-domain. Therefore, the frequency range for the “modal frequency” analysis must be selected based on the highest mode of interest. The reciprocal of the frequency range is equal to the sample rate in the time-domain. As illustrated in Chapter 3, a frequency range that is 16 times that of the highest mode of interest will produce a nicely shaped representation of the waveform for the highest mode in the time-domain response. This specification can be increased or decreased based on the needs of a particular research project. This would initially seem to be a severe limitation due to the dramatic increase in the frequency range required for the normal mode analysis compared to the typical specification. However, the results from Chapter 5 indicate that “zero-padding” can be used to obtain the desired sampling rate in the time-domain without causing a significant increase in the frequency range for the modal frequency response calculations. Applying a low-pass filter to the response also eliminates the possibility of aliasing. Therefore, time-domain resolution can easily be increased by simply increasing the size of the middle zero-valued portion of the linear spectrum in Matlab, such that the desired time resolution has little or no bearing on computational efficiency within NASTRAN.

The other important factor that affects the solution efficiency is the frequency spacing for the modal frequency response analysis. Based on the discussion in Chapter 3, the frequency resolution should be chosen based on the mode with the lowest $\eta * f$ value.

For most cases, if frequency resolution Δf is less than η^*f , the time-domain response will be relatively accurate in terms of amplitude, and since the Δf value was chosen based on the mode with the lowest η^*f value, the components of the time-domain waveform that correspond to the other modes will be accurately represented as well. However, since the fast Fourier transform generally requires uniform frequency spacing, an increase in computational efficiency could be obtained by deriving some of the frequency domain response from interpolation rather than direct calculation. An initial analysis could be performed using non-uniform frequency spacing with just enough frequencies to resolve the spectrum, and a secondary analysis performed to fill in the response at the required frequency spacing. While this would undoubtedly reduce the computation times, the modal frequency response calculations are not typically the most time-consuming part of the analysis, so the overall increase in computational efficiency will likely be small.

The final thing to remember regarding the selection of frequency resolution is that its reciprocal is the total length of the time-domain signal. When dealing with transient situations, a response and its decay are the central focus. Capturing the full decay may become a problem when frequency resolution becomes too large. So even though a particular frequency resolution selection is adequate for resolving the sharpest modal peak, it may not be small enough to capture the entire decay of the time-domain waveform. Thus, the frequency resolution should be chosen to balance the resolution of the sharpest peak and the overall length of the time signal.

Systems that are lossless or nearly lossless i.e. have very low damping, will most likely have very sharp modal peaks in the frequency-domain. A very small frequency resolution in a “modal frequency” analysis will be required to resolve these peaks and produce accurate amplitudes once transformed into the time-domain. Even after employing the techniques found in this thesis, there may be a point where the system is so close to being lossless that it becomes more computationally efficient to use NASTRAN’s “direct transient” solution sequence, rather than solve for a transformed frequency-domain solution where the frequency resolution is especially small.

The main accomplishment of the thesis is showing that transient calculations can be accurately performed by transforming harmonic frequency-domain calculations to the time-domain. Guidelines have also been developed to choose the sample rate and

frequency spacing to ensure accurate results. Thus, it should be possible to use existing frequency-domain methods for structural and acoustic computations and there is no need to develop time-domain versions of the codes. It also ensures that within the realm of transient problems, systems represented using complex-valued matrices can be resolved in the time-domain, and systems that are analyzed in the frequency-domain in general can also yield accurate time-domain responses.

References

1. *Femap w/NX Nastran, Version 9.31* (Siemens PLM, Plano, TX, 2007)
2. A.D. Nashif, D.I.G. Jones, and J.P. Henderson, *Vibration Damping* (Wiley, Canada, 1985), p. 148.
3. C.J. Martins, J.A.M. Carrer, W.J. Mansur, and F.C. Araújo. “On the Use of Pseudo-Forces to Consider Initial Conditions in 3D Time- and Frequency-Domain Acoustic Analysis.” *Computer Methods in Applied Mechanics and Engineering* 195 (2006): 4374-4382.
4. E. Barkanov, R. Rikards, C. Holste, and O. Täger. “Transient Response of Sandwich Viscoelastic Beams, Plates, and Shells under Impulse Loading.” *Mechanics of Composite Materials* 36 (2000): 367-378.
5. A. Akay, M.T. Bengisu, and M. Latcha. “Transient Acoustic Radiation from Impacted Beam-Like Structures.” *Journal of Sound and Vibration* 91(1983): 135-145.
6. J.D. Mehl and R.N. Miles. “Finite Element Modeling of the Transient Reponse of Viscoelastic Beams.” *SPIE* 2445(1995) 306-311.
7. K.J. Bathe, *Finite Element Procedures in Engineering Analysis* (Prentice-Hall, Englewood Cliffs, NJ, 1982).
8. K. Blakely, *MSC/NASTRAN, Basic Dynamic Analysis* (MacNeal-Schwendler, Los Angeles, 1993).
9. *Matlab* (The Mathworks, Inc., Natick, MA, 2009).
10. T. Gabrielson, *ACS 516 Class Notes*, (Penn State University, State College, PA, 2009), p. I-7 – I-14.

Appendix A: Summary of Transformed Frequency-Domain Solution Guidelines

Based on the analysis in this thesis, the following steps will yield accurate time-domain results from transformed modal frequency response calculations:

1. Perform a normal modes analysis to compute the resonance frequencies and loss factors over the frequency range of interest.
2. Compute the full frequency range required by multiplying the highest mode of interest by the number of points per wavelength desired in the time-domain.
3. Determine the frequency resolution required by finding the product of damping and frequency for each mode. Take the smallest value and set the preliminary frequency resolution to a convenient value less than this product.
4. Compute the time required for the dominant mode to damp out to a selected percentage of its original contribution using Equation 5.1.
5. If the reciprocal of the time value computed in step 4 is less than the frequency resolution value computed in step 3, set the frequency resolution to the step 4 value. If the step 4 value is greater than the step 3 value, set the frequency resolution to the step 3 value.
6. Perform a modal frequency analysis from 0 Hz to a selected value slightly higher than the frequency range of interest with frequency sample points at the interval specified in step 5.
7. Use the real and imaginary components of the modal frequency analysis output to construct the full linear spectrum from 0 Hz to the upper frequency required to resolve the highest mode of interest in the time-domain. The output data forms the first portion of the full spectrum, and once this data is inverted and the complex conjugate is taken, this new vector of data forms the final portion of the linear spectrum. The middle portion is filled in with zeros.
8. Take the inverse Fourier transform of the full linear spectrum formed in step 7 to compute the time-domain response.

Appendix B: Matlab Code

```
%%% This Matlab code illustrates the basic process of transforming
%%% Femap's frequency-domain output into time-domain data and making a
%%% comparison plot between the transformed frequency-domain data and
%%% Femap output time-domain data. This code and other simple
%%% variations of this code are used frequently to produce plots for
%%% this thesis.

%%% hingefreqreal = Femap output of the real part of the frequency-
%%% domain data

%%% hingefreqimag = Femap output of the imaginary part of the
%%% frequency-domain data

%%% hingetime = Femap output of time-domain data obtained through a
%%% "direct transient" analysis

%%% The following code combines the real and imaginary vectors into one
%%% complex number, mirrors the data across the y-axis, takes the
%%% complex conjugate, and then tacks it onto the end of the original
%%% data, forming one vector which represents the linear spectrum
%%% 'hingefull'. Then the Inverse Fourier Transform is taken to obtain
%%% the time-domain response, 'hingeifft'.

hingefreq = hingefreqreal + i*hingefreqimag;
hingeflip = flipud(hingefreq);
hingefull = [hingefreq; (conj(hingeflip(2:11250)))];
hingeifft = ifft(hingefull);

Ntime = 0:50000; %%% Number of points in Femap's time-domain output
delt = 0.0001; %%% Time resolution for Femap's time-domain output
forceerror = 20000; %%% Correction factor for forcing the system with a
%%% less than ideal impulse

Nshort = 0:8999; %%% Number of points in desired transformed
%%% frequency-domain vector
delft = 9000^-1; %%% Time resolutuion for transformed frequency-domain
%%% vector
N = 13500; %%% Number of points in the frequency vector
delf = (2/3); %%% Frequency resolution selected in femap
freqmult = N*delf; %%% Multiplication factor for transformed
%%% frequency-domain vector

%%% The following code produces a comparison plot between Femap output
%%% time-domain data, and transformed frequency-domain data.

plot(Ntime'.*delt,hingetime.*forceerror,Nshort'.*delft,(real...
(hingeifft3(1:9000)).*freqmult),'r','LineWidth',2);
legend('Time-Domain','Transformed Frequency-Domain');
xlabel('Time [s]');
ylabel('Response [m/N]');
grid
```


Appendix C: NASTRAN Input Deck for Figure 2.4 Time Analysis

```

INIT MASTER(S)
NASTRAN SYSTEM(319)=1
ID SingleDOF,Femap
SOL SEDTRAN
TIME 10000
CEND
  TITLE = Direct Transient Analysis
  ECHO = NONE
  DISPLACEMENT(SORT1,PLOT) = ALL
  ACCELERATION(SORT1,PLOT) = ALL
  SPCFORCE(SORT1,PLOT) = ALL
  SPC = 1
  DLOAD = 1
  TSTEP = 1
BEGIN BULK
$ *****
$   Written by : Femap with NX Nastran
$   Version   : 9.31
$   Translator : NX Nastran
$   From Model : C:\FEMAP931\SingleDOF.MOD
$   Date      : Fri Apr 02 11:16:27 2010
$ *****
$
PARAM,POST,-1
PARAM,OGEOM,NO
PARAM,AUTOSPC,YES
PARAM,MAXRATIO,1.E+8
PARAM,GRDPNT,0
CORD2C      1      0      0.      0.      0.      0.      0.
1.+FEMAPC1
+FEMAPC1    1.      0.      1.
CORD2S      2      0      0.      0.      0.      0.      0.
1.+FEMAPC2
+FEMAPC2    1.      0.      1.
$ Femap with NX Nastran Load Set 1 : Transient Load
PARAM,G,0.2865
PARAM,W3,1256.64
$ Femap with NX Nastran Function 1 : Unit Impulse
TABLED2      1      0.
+
+      0.      0.      1.E-5      0.5      2.E-5      1.      3.E-5      0.5+
+      4.E-5      0.      5.E-5      0.ENDT
TLOAD1      102      101      LOAD      1
FORCE       101      2      0      1.      1.      0.      0.
DLOAD       1      1.      1.      102
TSTEP       1      1499      1.E-5      1
$ Femap with NX Nastran Constraint Set 1 : Fixed
SPC1        1      123456      1
SPC1        1      23456      2
$ Femap with NX Nastran Property 1 : DOF SPRING Property
GRID        1      0      0.      0.      0.      0
GRID        2      0      1.      0.      0.      0
CELAS2      1      2910.      1      1      2      1      0.15
CONM2       2      2      07.371E-3      0.      0.      0.
2
+EL      2      0.      0.      0.      0.      0.
ENDDATA f4ec8938

```

Appendix D: NASTRAN Input Deck for Example Frequency Analysis

```

RESTART
ASSIGN MASTER='C:\FEMAP931\singl005.MASTER'
ASSIGN DBALL='C:\FEMAP931\singl005.DBALL'
NASTRAN SYSTEM(319)=1
ID SingleDOF,Femap
SOL SEMFREQ
TIME 10000
CEND
  TITLE = Modal Frequency Analysis
  ECHO = NONE
  DISPLACEMENT(SORT1,PLOT,REAL) = ALL
  ACCELERATION(SORT1,PLOT,REAL) = ALL
  SPCFORCE(SORT1,PLOT,REAL) = ALL
  SPC = 1
  DLOAD = 1
  METHOD = 1
  SDAMPING = 3
  FREQUENCY = 1
BEGIN BULK
/,1,999999
$ *****
$   Written by : Femap with NX Nastran
$   Version   : 9.31
$   Translator : NX Nastran
$   From Model : C:\FEMAP931\SingleDOF.MOD
$   Date      : Fri Apr 02 11:46:11 2010
$ *****
$
PARAM,POST,-1
PARAM,OGEOM,NO
PARAM,AUTOSPC,YES
PARAM,MAXRATIO,1.E+8
PARAM,GRDPNT,0
CORD2C      1      0      0.      0.      0.      0.      0.
1.+FEMAPC1
+FEMAPC1     1.      0.      1.
CORD2S      2      0      0.      0.      0.      0.      0.
1.+FEMAPC2
+FEMAPC2     1.      0.      1.
EIGRL       1              10      0              MASS
$ Femap with NX Nastran Load Set 1 : Transient Load
$ Femap with NX Nastran Function 1 : Viscous Damping
TABDMP1      1      G
+            0.      0.      100. 0.14325      200. 0.2865ENDT
$ Femap with NX Nastran Function 2 : Transient Load
TABLED2      2      0.
+            0.      1.      200.      1.ENDT
RLOAD2      102      101              2              LOAD
FORCE       101      2      0      1.      1.      0.      0.
DLOAD       1      1.      1.      102
FREQ1       1      10.      10.      159
FREQ        1 100.001
$ Femap with NX Nastran Constraint Set 1 : Fixed
SPC1        1 123456      1
SPC1        1 23456      2
$ Femap with NX Nastran Property 1 : DOF SPRING Property
GRID        1      0      0.      0.      0.      0
GRID        2      0      1.      0.      0.      0
CELAS2      1 2910.      1      1      2      1      0.15

```

CONM2	2	2	07.371E-3	0.	0.	0.	+EL
2							
+EL	2	0.	0.	0.	0.	0.	
ENDDATA	26a2c571						